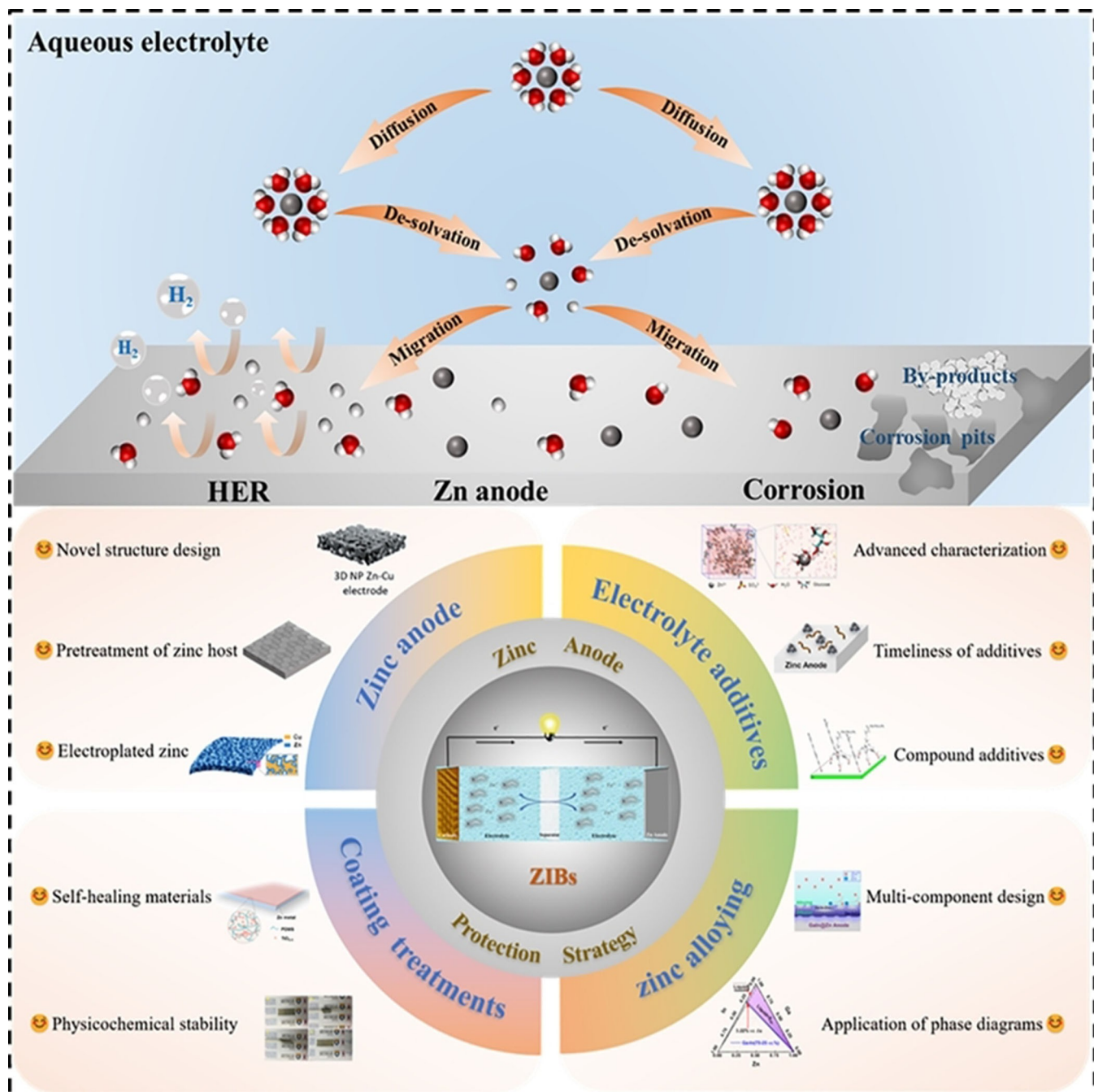


VIP Very Important Paper

www.batteries-supercaps.org

Towards Understanding the Corrosion Behavior of Zinc-Metal Anode in Aqueous Systems: From Fundamentals to Strategies

Qian Li,^[a, c] Lishun Han,^[a] Qun Luo,^[a] Xiaoyu Liu,^{*[b]} and Jin Yi^{*[b]}

Owing to the properties of cost-efficient, high-energy density and environmental friendliness, rechargeable aqueous zinc-metal batteries (RAZMBs) are promising candidates for the next generation metal-based batteries in large-scale energy storage systems. However, the practical applications of RAZMBs are severely limited due to the presence of inevitable side reactions referring to zinc corrosion and hydrogen evolution reaction (HER) occurring at the electrode-electrolyte interface. The uninterrupted interfacial side reactions at the expense of continuous capacity fading and reduced reversibility of zinc are

required to give more attention to mitigate them. Given the above concerns, in this review, the fundamental principles of corrosion thermodynamics and kinetics of zinc electrodes in aqueous media are elucidated. Furthermore, the recent optimization strategies targeting enhanced stability of zinc electrodes are reviewed including electrolyte additives, zinc alloying, electrodeposited Zn and coating treatments. Finally, considering the current main research orientations, some perspectives are provided to facilitate the development of future applications of zinc anodes.

1. Introduction

In recent years, the market has been successfully occupied by various advanced energy storage systems as the demand for energy resources has increased.^[1–11] Rechargeable aqueous zinc-based batteries (RAZMBs) have proven to be one of the most promising candidates in a variety of application scenarios.^[12–17] Compared with lithium-ion batteries using conventional organic electrolytes, RAZMBs have been received widespread attention due to their advantages in terms of safety and economic efficiency. Because of the environmental friendliness, low cost and high theoretical capacity (820 mAh g^{-1} and 5855 mAh cm^{-3}), metallic zinc has been widely used as anode material.^[14,16,18–22] The current electrolytes could be classified into alkaline, neutral and mild acidic electrolytes. In recent years, rechargeable aqueous zinc-ion batteries used neutral or mild acidic electrolytes (e.g., Zn-MnO₂ batteries) and alkaline electrolytes (e.g., Zn-air batteries) have achieved decent developments.^[23–27] However, zinc anode still faces grand challenges, which seriously hinder the large-scale application. Besides the issues such as dendrites and deformation, zinc corrosion is a crucial issue, which is the main cause of the decrease in the Coulombic efficiency of RAZMBs. Similar to other active metals, zinc is subject to be corroded in the electrolytes, resulting in uneven surface morphology and the generation of inert by-products covering the zinc surface. Subsequently, it causes low Coulombic efficiency. In addition, zinc corrosion is accompanied by the hydrogen evolution reaction (HER). The hydrogen gas could cause the battery to

swell, bulge, and even explode. Consequently, the corrosion problems of zinc anode are required to be solved urgently.^[28–31]

Currently, alkaline electrolytes, such as KOH, NaOH and LiOH, have been widely used. Among them, KOH has attracted considerable attention due to its high solubility, high ionic conductivity and fast reaction kinetics. However, zinc anode is still restricted owing to the severe dendrites and passivation in alkaline solutions. In this context, neutral and mild acidic electrolytes are in the limelight. Among them, ZnSO₄ solution and Zn(CF₃SO₃)₂ have drawn increasing research attention, both of which deliver a wide electrochemical window and stable structure (Figure 1a). Furthermore, the larger volume of CF₃SO₃[–] ions can weaken the solvation effect of zinc ions, accelerate the transport and charge transfer rate of zinc ions, together with effectively inhibit the side reactions.^[32] Compared to the high cost of Zn(CF₃SO₃)₂, ZnSO₄ becomes more competitive due to its lower cost and faster ion transport kinetics.^[33] The current use of electrolytes in zinc-ion batteries is shown in Figure 1(b–d).

Zinc corrosion can be classified as self-corrosion and electrochemical corrosion. In alkaline electrolytes, the self-corrosion of zinc dominates because the standard redox potential of Zn/ZnO (-1.26 V vs. SHE) is lower than the one of HER (-0.83 V vs. SHE), while in neutral and mild acidic electrolytes, the electrochemical corrosion of zinc refers to the dissolution of zinc anode. During the discharge process, by-products are formed through the complexation of zinc ions with electrolyte anions (e.g., SO₄^{2–}, Cl[–], etc.).^[34] Zinc corrosion is influenced by various factors such as the component and morphology of zinc electrodes, the composition, concentration and pH value of electrolyte, as well as the operating conditions of batteries.^[35]

In this review, the fundamentals of zinc corrosion in alkaline and mild acidic electrolytes are elucidated, furthermore, the corrosion behavior of zinc is discussed in depth. Meanwhile, the recent advances in retarding zinc corrosion are summarized emphatically. Finally, the future promising strategies of zinc anode for aqueous zinc-ion batteries are prospected.

[a] Prof. Q. Li, L. Han, Prof. Q. Luo

State Key Laboratory of Advanced Special Steels & Shanghai Key Laboratory of Advanced Ferrometallurgy & School of Materials Science and Engineering
Shanghai University
Shanghai 200444, China

[b] Prof. X. Liu, Prof. J. Yi

Institute for Sustainable Energy/College of Sciences
Shanghai University
Shanghai 200444, China
E-mail: xiaoyuliu@shu.edu.cn
jin.yi@shu.edu.cn

[c] Prof. Q. Li

National Engineering Research Center for Magnesium Alloys
Chongqing University
Chongqing 400044, China



Supporting information for this article is available on the WWW under
<https://doi.org/10.1002/batt.202100417>

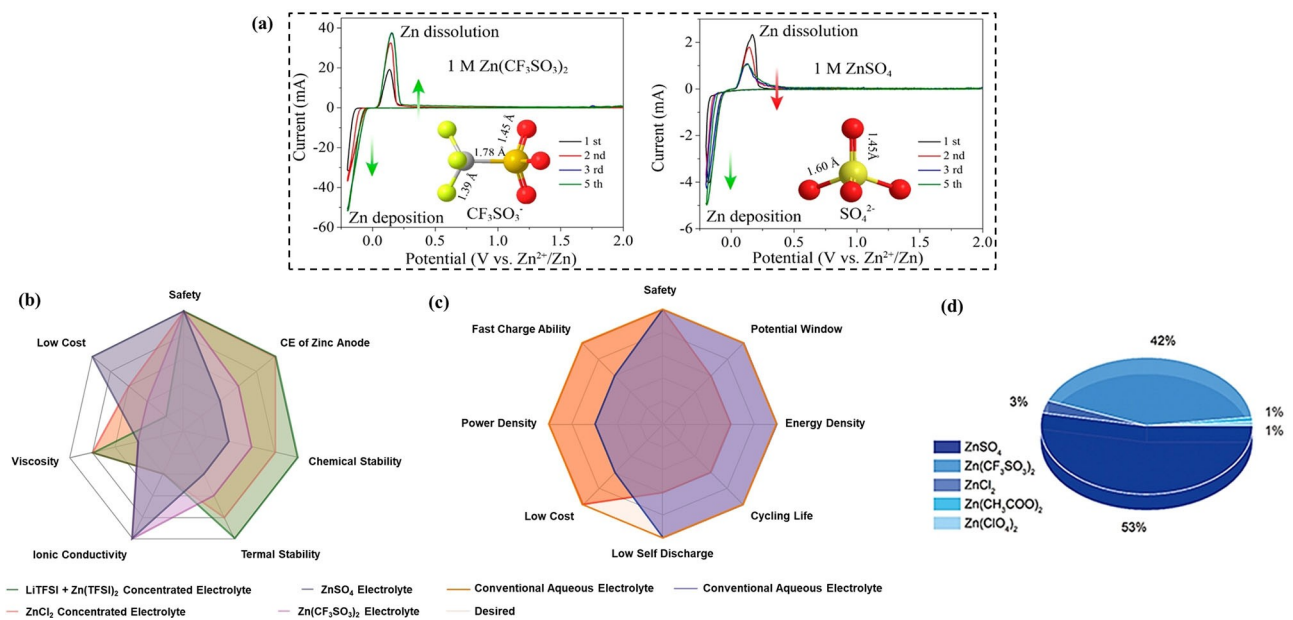
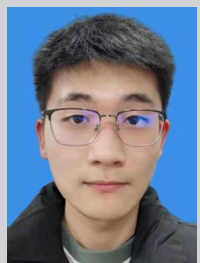


Figure 1. a) Cyclic voltammograms of Zn electrode in both types of electrolytes. Reproduced with permission from Ref. [32]. Copyright (2016) American Chemical Society. b) Radar chart comparison of various electrolytes and c) the performance of conventional and concentrated aqueous electrolytes. d) The usage of electrolytes of aqueous zinc-ion batteries. Reproduced with permission from Ref. [33]. Copyright (2021) Shanghai Institute of Organic Chemistry, Chinese Academy of Sciences.



Qian Li is presently Professor in the Department of Materials Science, College of Materials Science & Engineering, Chongqing University. He received his Ph.D. from University of Science and Technology Beijing in 2004. Prior to joining Chongqing University in 2021, he has been working at Shanghai University, China, rising through the ranks to a senior full professor. From 2012 to 2013, he worked as a distinguished senior visiting scientist and faculty at Oak Ridge National Laboratory in the US. His current research interests include thermodynamics and kinetics in materials science and new energy storage materials.



Lishun Han received his bachelor's degree in the College of Materials Science and Engineering from Chongqing Jiaotong University in 2020. He currently is a master student in Prof. Qian Li's group in the School of Materials Science and Engineering, Shanghai University. His research interests focus on aqueous zinc-ion batteries.



Qun Luo, Ph.D., Shanghai University. Research interests focus on thermodynamic and kinetic mechanism of phase transformation in magnesium and aluminum alloys. She is the fellow of China Magnesium Alloy Youth Committee and youth editor of Journal of Magnesium and Alloys, Rare Metals, International Journal of Minerals, Metallurgy and Materials, etc. She has got the Young Elite Scientists Sponsorship Program By CAST, Shanghai "Rising-Star" and "Chenguang" Programs.



Xiaoyu Liu currently works in Shanghai University, China. She received her B.S. and Ph.D. degree from Fudan University in 2011 and 2016, respectively. Her research interests involve electrochemical functional materials and their application in lithium-ion batteries and zinc-ion batteries.



Jin Yi obtained his Ph.D. from Fudan University in 2014, and later worked as a postdoctoral researcher in National Institute of Advanced Industrial Science and Technology (AIST), Japan. He currently works in Shanghai University. His research interests focus on advanced materials and their application in various batteries including zinc-ion batteries, solid state batteries and metal-air batteries.

2. Corrosion Behavior of Zinc Electrodes

2.1. Endogenous and exogenous causes of zinc corrosion

Commercial zinc flakes or foils are used as the anode for the aqueous zinc-based batteries. Typically, the raw zinc foil needs to be subjected to a series of manufacturing processes, after which a final shearing step is required to create the commercial zinc foil (Figure 2a and b). Finally, the zinc foil would be employed to assemble the battery after the additional cutting to achieve the desired shape.^[36] As zinc is a relatively soft metal, the manufacturing process often leaves various types of surface defects on the final zinc foil surface, which significantly reduces the cycling stability of the zinc foil.^[36–38] Zinc electrodes with non-uniform surfaces present different potentials in different regions, so that the galvanic cell corrosion can form on the surface of anodes along with converting chemical energy into electrical energy and deteriorating the battery performance in aqueous electrolyte environments.^[30,39,40] The strategies involving chemical polishing have been used to treat the zinc surface and obtain a uniform ridge-like structure, which can optimize the cycling performance of batteries (Figure 2c and d). However, the further exploration of surface modification techniques adapted to commercial production is still needed.^[22]

The electrochemical corrosion and HER during cycling are closely related to the deposition behavior of Zn^{2+} , which undergoes three steps: (1) the diffusion of Zn^{2+} from the electrolyte to electrode interface, (2) the de-solvation of Zn^{2+} from the anode surface, and (3) the migration of Zn^{2+} at the surface.^[41,42] As the decisive speed step, the de-solvation behavior of Zn^{2+} is critical for the whole electrochemical reactions. Limited by the aqueous environment, Zn^{2+} and H^+ exist as hydrated structures, namely $Zn(H_2O)_6^{2+}$ and H_3O^+ ,

respectively.^[41] $Zn(H_2O)_6^{2+}$ features a regular octahedral structure in aqueous solutions, and Zn^{2+} would be electroplated to form Zn after the desolvation process. During the charging process, Zn^{2+} needs to undergo the desolvation process to be plated as Zn, however, the side reaction of water decomposition accompanies the desolvation process. Water is decomposed into H^+ and OH^- , the steps of HER are shown in Equations (1)–(3):^[43]

Volmer step:



Tafel step:



Heyrovsky step:



In mild acidic and alkaline electrolytes, the decisive steps for hydrogen precipitation are Equations (1) and (2), respectively.^[43] Finally, H_2 can be produced, which comes from the discharge reaction of H_3O^+ .^[41] The formation of corresponding by-products is inevitable along with the formation of OH^- left through the decomposition of water (Figure 2e). The essence of zinc corrosion in various electrolytes is the complexation reaction of dissolved Zn^{2+} with H_2O molecules and anions in zinc salts, leading to the formation of different corrosion by-products, such as $Zn_4SO_4(OH)_6 \cdot xH_2O$,^[12,44–46] $Zn_5Cl_2(OH)_8 \cdot H_2O$,^[47] $Zn_x(CF_3SO_3)_y(OH)_{2x-y} \cdot xH_2O$,^[48] and other alkaline zinc salt complexes. The corrosion by-products differ depending on the concentration and size of the solute molecules.^[32,49] Although

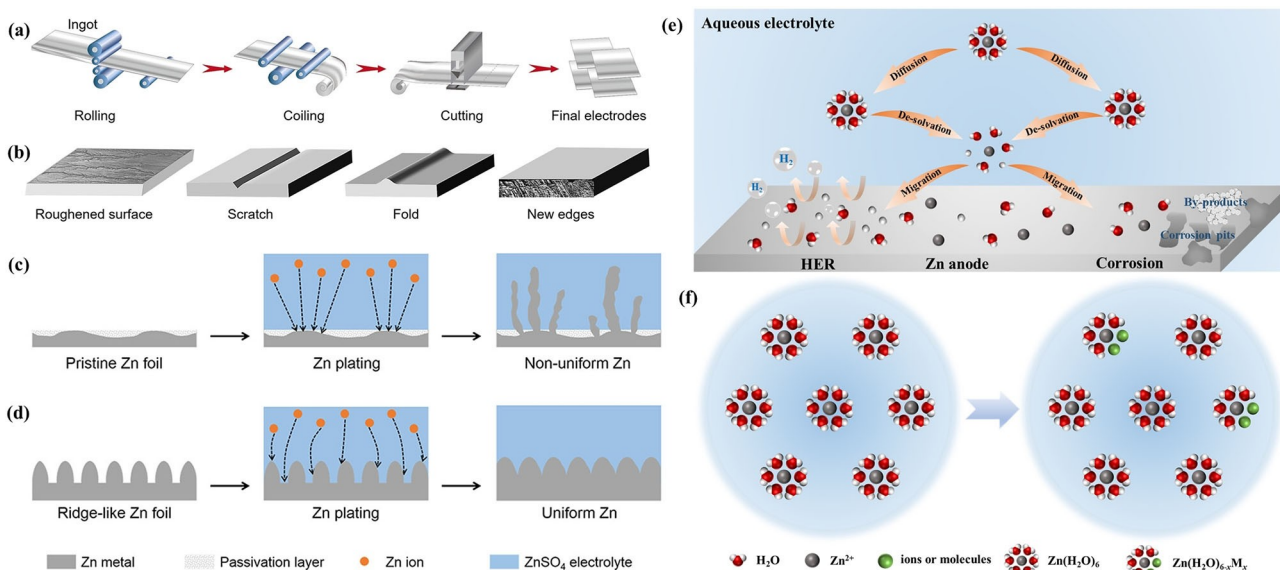


Figure 2. Schematic diagrams of a) the manufacturing process of commercial zinc foil and b) the surface defects created on the zinc foil. Reproduced with permission from Ref. [36]. Copyright (2021) American Chemical Society. Schematic illustrations of the zinc plating process on c) the pristine zinc foil electrode and d) the zinc foil with ridge-like structure. Reproduced with permission from Ref. [22]. Copyright (2020) American Chemical Society. e) Schematic illustration of the relationship between the deposition behavior of Zn^{2+} and side reactions. f) Schematic diagram of the inhibition of the solvated structure of Zn^{2+} .

the inert product layer covers the zinc surface, its internal loose porous-like pores allow the transport of zinc ions, the corrosion products fail to act as a passivation layer like ZnO in alkaline electrolytes, and further corrosion of zinc is not retarded.^[50] Except for ZnSO₄ aqueous electrolyte, the corrosion in other aqueous electrolytes has been little studied, the solvated structures of Zn²⁺ are present in all electrolytes. Since water is known to be the culprit of Zn corrosion and HER, it is logical to minimize the content of free and active water, therefore, the control of the solvated structure of Zn²⁺ would be an ideal method.^[51] The disadvantages caused by aqueous electrolytes have been reported to be mitigated by increasing the salt concentration or adding organic additives. The increase in salt

concentration and the introduction of organic ligands disrupt the solvated structure of Zn²⁺ and reduce the solvent water content (Figure 2f), but the excessive cost limits their development, consequently, the low-cost and efficient methods are required to be explored.^[52-55]

The working principle of zinc-based batteries based on various aqueous electrolytes is shown in Figure 3(a).^[19] Although the charging process is approximately the same for both systems, the discharge process differs widely with uncontrollable side reactions and the generation of by-products. Zinc anodes suffer self-corrosion and electrochemical corrosion in various aqueous electrolytes together with HER during the shelving and working period of batteries, respec-

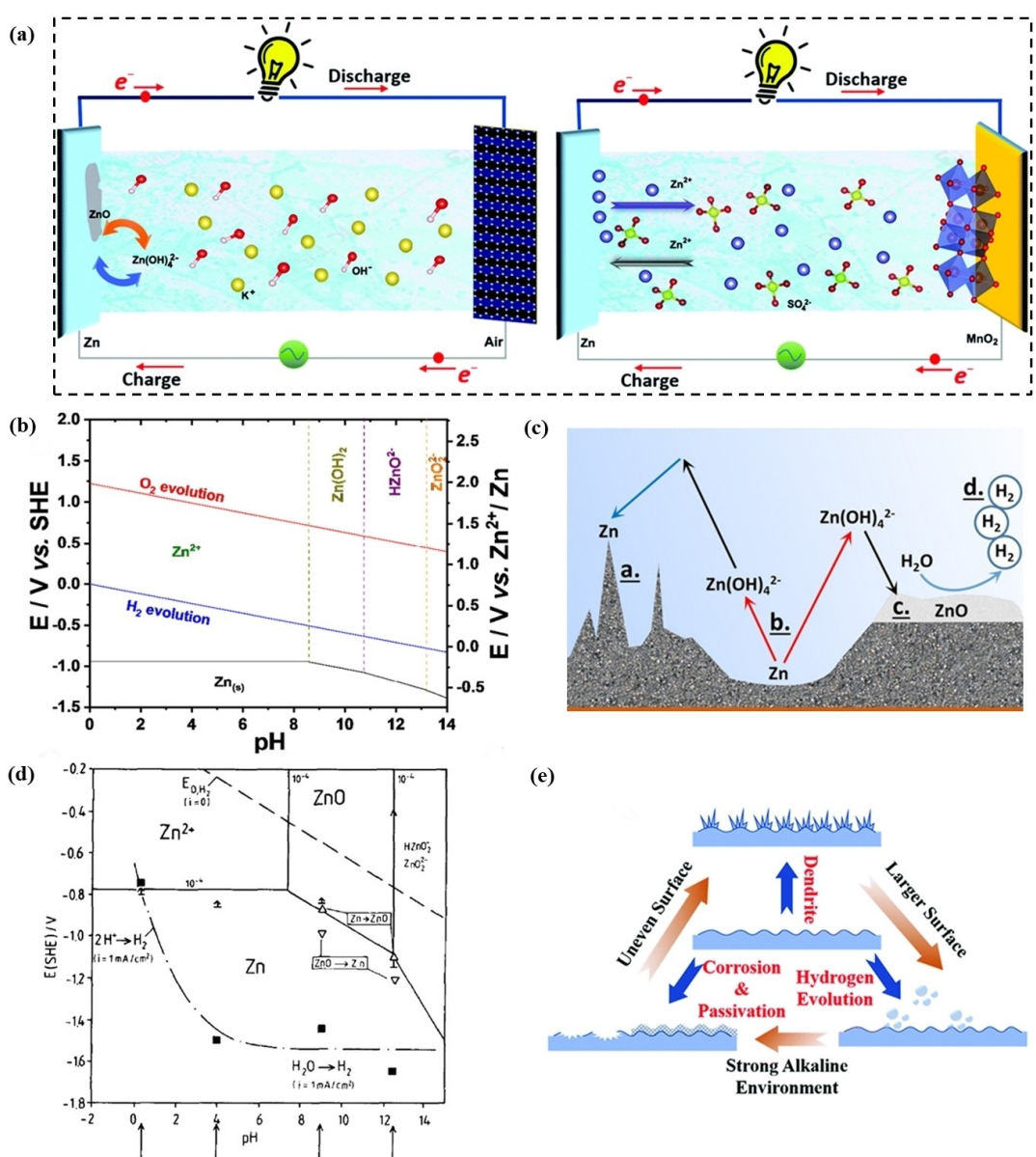


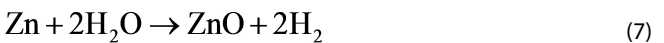
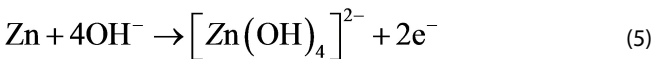
Figure 3. a) Schematic illustration of aqueous zinc-metal batteries used alkaline and mild acidic electrolyte. Reproduced with permission from Ref. [19]. Copyright (2020) Royal Society of Chemistry. b) Pourbaix diagram of Zn. Reproduced with permission from Ref. [58]. Copyright (2018) American Chemical Society. c) Schematic illustration of the zinc electrode surface state during cycling. Reproduced with permission from Ref. [59]. Copyright (2016) Wiley-VCH. d) Pourbaix diagram of Zn with HER overpotential considerations. Reproduced with permission from Ref. [72]. Copyright (1990) Elsevier. e) The interaction of unresolved issues occurring on the zinc anode. Reproduced with permission from Ref. [74]. Copyright (2021) Royal Society of Chemistry.

tively. Although zinc displays a high hydrogen evolution overpotential, HER is inevitable in aqueous solutions due to a series of factors such as surface morphology of zinc electrode, electrolyte composition, change of the pH value during cycling and so on.^[56] HER also leads to an increase in the local pH of electrolyte, which provides an important source of OH⁻ in the electrolyte and leads to the over-consumption of electrolyte.^[57]

Although aqueous electrolytes are thermally favorable for zinc corrosion, zinc corrosion is a cathodically controlled process. The rate of cathodic hydrogen precipitation limits the rate of zinc corrosion. Therefore, the overpotential for zinc corrosion is highly correlated with the HER reaction in aqueous electrolytes with different pH.^[43] The evolution of the chemical behavior of zinc in aqueous solutions under different pH is shown in Figure 3(b). The HER would take place on the zinc surface under various pH ranges.^[58] Above a special pH value (pH~8), the hydroxides and oxides would be produced during discharging, leading to severe dendritic growth and passivation on the zinc surface.^[59] As a result, the capacity of the battery is limited on account of the reduction of active material, which in turn reduces the corresponding discharge capacity. It can also be found from the Pourbaix diagram that the generation of discharge products can be avoided by changing the pH of electrolytes. As demonstrated in Figure 3(b), zinc forms Zn²⁺ directly during discharge when pH<7. In addition, the critical potential for HER on the Zn surface decreases with increasing pH, which indicates that HER is more likely to occur in acidic solutions.^[60] Therefore, zinc is unstable in aqueous solutions based on the thermodynamic perspective analysis. In alkaline solutions, zinc is stable in the form of HZnO₂⁻ or ZnO₂²⁻, but when the pH value ranges from 8.5 to 10.5, the zinc surface would be covered by Zn(OH)₂ acting as a passivation layer, inhibiting the dissolution of zinc. In acidic solutions, zinc is stable in the form of Zn²⁺. The corrosion behavior of zinc in aqueous solutions with different pH values is specifically elucidated in the following sections.

2.2. Corrosion behavior of zinc in alkaline electrolyte

Generally, zinc is oxidized to Zn²⁺ during discharge, and the resulting electrons are transferred to the cathode via an external circuit. In alkaline media, the oxidized Zn²⁺ combines with OH⁻ to form Zn(OH)₄²⁻ complexes due to a large number of hydroxide ions in the vicinity of the zinc electrode. These complexions not only diffuse away from the surface due to the concentration gradient, leading to the loss of active material, but once the local solubility limit of the salt is reached, the complexions precipitate as ZnO are obtained [Eqs. (5) and (6)], leading to the dendritic growth and passivation of zinc, which impairs the rechargeability of batteries (Figure 3c).^[38] The HER [Eq. (4)] and oxidation reaction [Eq. (5)] occur simultaneously on the zinc electrode when employing KOH electrolyte, and the total reactions are presented in Eq. (7).



Thermodynamically, it is known that zinc is unstable in alkaline solutions and dissolves itself while releasing hydrogen. Also, from the kinetic point of view, the difficulty in zinc corrosion is subsistent because of the relatively higher HER overpotential of zinc.

2.3. Corrosion behavior of zinc in mild acidic electrolyte

The neutral or mild acidic electrolytes used in zinc-based batteries mainly include Zn(CH₃COO)₂,^[61–63] ZnSO₄,^[64–66] Zn(TFSI)₂,^[67] Zn(CF₃SO₃)₂^[68–70] and other salt solutions containing Zn²⁺ with high ionic conductivity. In mild acidic electrolyte (3 < pH < 7), a passivation layer is difficult to be produced, while zinc is stable in the form of Zn²⁺. Through employing mild acidic aqueous solutions, such as ZnSO₄ or Zn(CF₃SO₃)₂, the reversible zinc plating/stripping processes can be carried out, enabling the reversible charge/discharge processes of the battery. The reactions taking place on the zinc electrode are presented in Equations (8) and (9):

Discharge:

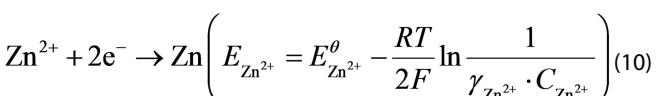


Charge:

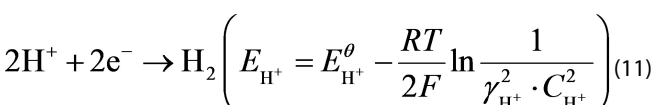


Taking ZnSO₄ electrolyte as an example, the reactions occurring on the zinc electrode and the corresponding electrode potentials are presented in Eqs. (10)–(13):^[71]

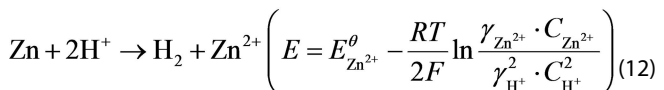
Deposition:



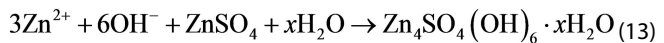
HER:



Corrosion:



Side reaction:



where E is the potential, γ denotes the activity, C stands for the concentration and the other physical parameters represent specific values. Because of HER and zinc corrosion, the constant consumption of H^+ synchronizes with the side reactions caused by the remaining OH^- , leading to no significant change in the pH value of the electrolyte. Nevertheless, in neutral or mild acidic electrolytes, the zinc deposition reaction is kinetically more vigorous than HER because of the high overpotential, slow hydrogen reaction kinetics and low H^+ activity. In fact, HER is almost inevitable due to the persistent variation of the shape of the zinc electrode and the local pH of the electrolyte during cycling.

As predicted by the Nernst equation and Pourbaix diagram, the hydrogen evolution overpotential can be increased by increasing the pH value of the solution. For example, the hydrogen evolution overpotential is calculated to be -0.59 V (vs. SHE) for the pH~10 solution, while it is -0.236 V (vs. SHE) for the pH~4 solution (Figure 3d), implying that the HER is inclined to take place during discharge process in solutions with low pH value.^[72] Indeed, the hydrogen evolution overpotential is much higher than the zinc reduction potential (-0.76 V vs. SHE), which suggests that the HER occurs thermodynamically before zinc deposition. As it is well known, different metals exhibit different kinetic overpotentials for surface reactions such as HER, and there is often a hysteresis in the kinetics of HER, considering factors such as H^+ activity in solutions and the state of the electrode surface. Fortunately, zinc has a higher electrode potential compared to other reactive metals, which indicates that the HER is more difficult to occur at the zinc surface.^[72,73] Therefore, the hydrogen precipitation overpotential can be increased through suitable approaches, making it possible for zinc deposition to occur first. It is worth noting that external factors, such as temperature changes and system perturbations, can also affect the degree of reduction for the hydrogen precipitation overpotential. Subsequently, the interference is suggested to be avoided as much as possible in the practical application. In addition, if there are other metallic impurities with a low overpotential of HER on the zinc surface, a local primary cell with zinc as the anode will be formed in this case, which also causes zinc corrosion. Moreover, there is a close relationship between zinc corrosion and other side reactions (Figure 3e). For instance, the increased specific surface area of zinc dendrites will promote zinc corrosion and HER, and the inhomogeneous surface formed by corrosion will, in turn, promote the growth of zinc dendrites. Consequently, how to effectively suppress the side reactions is required large efforts in the future.

3. Optimization Strategies for Corrosion Inhibition

The zinc corrosion and HER would take place in both alkaline and mild acidic electrolytes, inevitably causing the waste of zinc anodes and reducing the reversibility of zinc. Considerable efforts have been made in recent years to develop zinc anode, which mainly involves the developments on electrolyte, zinc anode and their interface. Considering the limited space of this review, large attention will be paid to the recent achievements in zinc anode through the strategies including electrolyte additives and zinc modifications, such as zinc alloying and coating treatments. The corresponding recent advances are summarized and discussed, meanwhile, several insights with potential applications are also presented. It is briefly explained here that zinc dendrites and zinc corrosion are causally related to each other, and because of their special relationship, the following will inevitably involve describing zinc dendrites to deepen the understanding of the basic principles of zinc corrosion.

3.1. Electrolyte additives

As a promising strategy, the employment of electrolyte additives can effectively address the problems of zinc corrosion and HER. It is found that the electrolyte additives not only inhibit zinc corrosion but also suppress zinc dendrites growth and passivation formation, which could be of potential benefit in enabling high-performance zinc-based batteries in the future. Generally, the electrolyte additives can be divided into organic and non-organic additives. Moreover, electrolyte additives can also be divided into two categories.^[75] The additives can be used to regulate the crystal growth orientation of the zinc surface. The underlying cause is originated from the change of surface energy. Furthermore, additives can be employed to control the structure of anode surface film. As it is well known, the small angle between crystal orientation and the substrate is detrimental to dendrites formation, however, the interfacial reactivity and corrosion tendency increase inversely following the increase of surface area. The zinc deposition orientation would be changed due to the decrease of crystal surface energy, which is caused by specific interactions of additive molecules or ions with different crystalline surfaces. Moreover, the adsorption film consisting of additive molecules or ions on the electrode surface can physically isolate the electrolyte from direct contact with the electrode surface, leading to corrosion inhibition. In addition, an effective strategy has been proposed to construct the H-bonding with free water to reduce the reactivity of solvent water by adding certain functional additives. According to the various function mechanism of additives, the recent research achievements are described below.

3.1.1. Effects of additives on electrodeposition

Pre-zinc surface texture representing the preferential orientation of zinc electrodeposition shows an important influence on the later zinc electrodeposition morphology, which plays a key role in the corrosion resistance of zinc anodes. Generally, the larger angle exists between substrate and zinc crystallographic growth direction, the more favorable dendrites growth is exhibited, which is the trigger for the aggravated zinc corrosion behavior.^[76,77] The fast zinc corrosion tends to take place on zinc surfaces with crystallographic orientations of (100) and (110) crystal planes, where the crystal growth direction is at an angle of approximately 70°–90° to the substrate. The crystal planes with low corrosiveness are (002), (103), (105), and the angle between crystal growth direction and the substrate is 0°–30°, which are favorable for corrosion inhibition and zinc deposition. It can be widely observed that the zinc crystallographic orientations are (114), (112), (102) and (101) crystal planes (Figure 4), which are the typical zinc electrodeposition on the commercial zinc foil.^[75] In order to obtain a zinc anode with decent corrosion resistance, controlling the zinc growth direction in a small angle range is a crucial consideration. The zinc growth direction is associated with surface energy. The lowest surface free energy of zinc crystal is the basal (002) plane, owing to its compactness.^[78]

To date, various electrolyte additives have been proposed to mitigate the corrosion of zinc in the electrolyte by changing the direction of zinc growth, especially on the (002) crystal plane. The formation of (002) crystal surface is facilitated by adding some typical inorganic additives.^[76] In the alkaline zincate solutions, the formation of complex zinc electrodeposits

is regulated by various additives (Figure 5a). The ratio of the (002) crystal plane increases with the increase of boric acid addition. Similarly, the growth of zinc dendrites on the (101) crystal plane is inhibited by tin oxide and indium sulfate additives, promoting zinc electrodeposition on the (002) or (103) crystal plane (Figure 5b). The corrosion rate of zinc can be decreased 11 times with the addition of indium sulfate, which is consistent with the results of the float charge current (Figure 5c). In addition, the capacity retention after 1000 charge/discharge cycles is significantly improved compared to one of the batteries containing commercial zinc. These remarkable improvements are attributed to the elaborate fabrication of zinc anodes with adaptive crystallographic orientation and morphology (Figure 5d). Furthermore, the metal ion additives including Pb also regulate the preferential growth of zinc crystals on the (002) crystal plane (Figure 5e).^[81] The potential causes of zinc surface crystallographic orientation affecting deposited morphology can be summarized as follow: zinc is a hexagonal close-packed structure (hcp), and the (001) crystal plane is a stable close-packed substrate that is detrimental to the formation of dendrites. For this reason, crystallographic planes, for example (002), (103), (105), approximately paralleling to (001) inhibit dendrites growth. Instead, crystallographic planes perpendicular to (001) are inclined to dendrites generation, such as (100) and (110). That means, the easier the zinc electrode is to be corroded once the angle between the (001) substrate of the electrode surface and crystal planes is increased.

Recently, extensive attention has been drawn to investigating the effects of organic additives on zinc deposition. For example, Sun et al.^[82] deeply investigated the effects of sodium

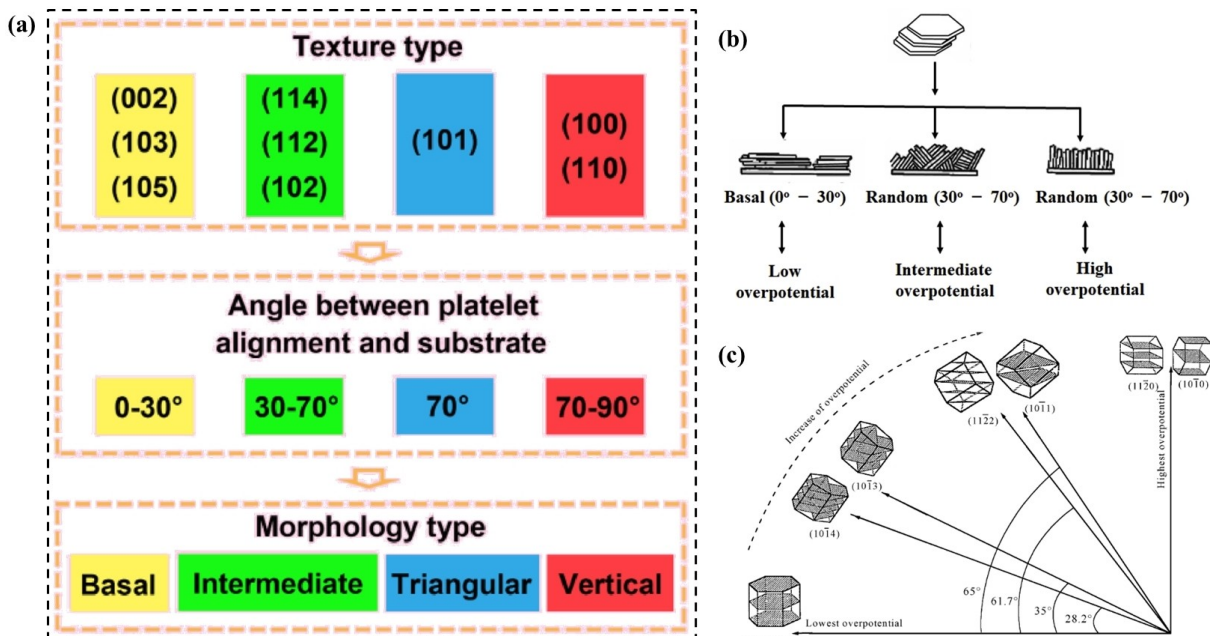


Figure 4. a) The correlation of the texture type, angle and morphology type. Reproduced with permission from Ref. [75]. Copyright (2020) Elsevier. b) The growth mechanisms of zinc deposition. Reproduced with permission from Ref. [79]. Copyright (2017), Elsevier. c) The relevance of the overpotential and the angle (between the preferred oriented plane and the (0002) plane). Reproduced with permission from Ref. [80]. Copyright (2008) Elsevier.

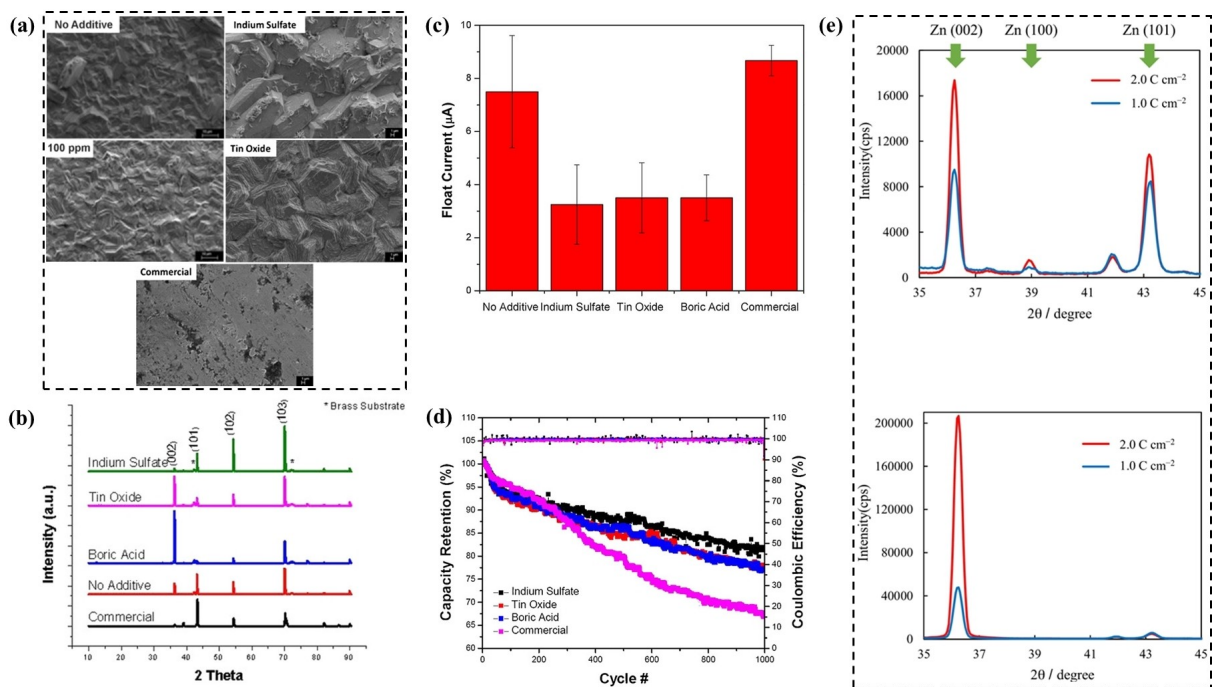


Figure 5. a) Electrodeposition morphology of zinc with various additives. b) XRD patterns of electroplated zinc with indium sulfate, tin oxide, boric acid and commercial zinc foil. c) Float current and d) cyclability of the battery with synthesized zinc. Reproduced with permission from Ref. [76]. Copyright (2018) Wiley-VCH. e) XRD patterns of Zn with Pb additive. Reproduced with permission from Ref. [81]. Copyright (2017) Elsevier.

dodecyl sulfate (SDS), thiourea (TU), polyethylene-glycol (PEG 8000) and cetyltrimethylammonium bromide (CTAB) on zinc deposition in mild acidic electrolytes. According to the XRD patterns results, it is found that different crystallographic orientations can be observed through the participation of various electrolyte additives. The (101) and (103) crystal planes can be observed for commercial zinc foil in the blank electrolyte. Compared to the (101) crystal plane, the (103) crystal plane shows a smaller angle with the substrate, and the crystals are less likely to grow into dendrites, exhibiting better corrosion resistance. From Figure 6(a), it can be found that the meritorious growth on the (101) crystal plane for Zn-CTAB, Zn-SDS, and Zn-TU are observed, but the corresponding peak intensities are all lower than those of Zn-No. While Zn is subjected to be deposited on the (103) crystal plane in Zn-PEG. The presented results demonstrate that zinc growth can be controlled through the participation of electrolyte additives. The zinc growth on the (101) crystal plane is inhibited, while the zinc growth on (002) and (103) crystal planes are facilitated. The Tafel fitting results show that the corrosion rate of zinc anodes can be decreased through employing additives, and the corrosion inhibition efficiency is ranked as follows: Zn-CTAB < Zn-PEG < Zn-SDS. However, the high corrosion rate of Zn-CTAB is associated with the increased surface area (Figure 6b and c). The unique function of surfactants that change the morphology of zinc anode can be ascribed to the formation of an organic protective layer on the zinc surface, resulting in the reduction of the active center and nucleation rate on the zinc surface.^[78,83]

The organic additive is involved in the formation of a characteristic morphology, which is deposited on the metallic

electrode surface. For example, Hao et al.^[84] assessed the effect of sodium dodecylbenzene sulfonate (SDSB) on the zinc anode and LiFePO₄ (LFP) cathode of the LFP/Zn battery. Figure 7(a-c) shows the morphology of commercial zinc foil and electrodeposited zinc electrodes with additives or not, respectively. During charging and discharging, serious corrosion occurs on the surface of zinc foil, resulting in low Coulombic efficiency and zinc reversibility of the battery. The results in Figure 7c show that no obvious corrosion can be found on the zinc surface, which helps improve the Coulombic efficiency and cycling stability. The additives promote the wettability of the zinc foil and facilitate zinc nucleation as well, resulting in a uniform electrodeposited surface (Figure 7d and e). This affects the kinetic process of electron transfer and increases the competition between nucleation and growth. Moreover, it is found that the highest intensity peak of the electrodeposited zinc appears at about 42° when the additives are absent, indicating that the majority of the zinc crystal growth is in the (101) crystal plane. Although the major (101) peak is also found when the additives are used, the variation in the XRD patterns indicates that the growth of zinc crystals is influenced by the additives, promoting the growth of zinc in the (100) and (110) crystal planes (Figure 7f). The decreased polarization and improved cycling lifetime achieved by the employment of additive have been confirmed in polarization curves of Zn symmetric cells (Figure 7g). It is presumed that zinc growth direction is affected by the affinity of the electrolyte-containing additives to the zinc surface, which is a consequence of surface energy differences.

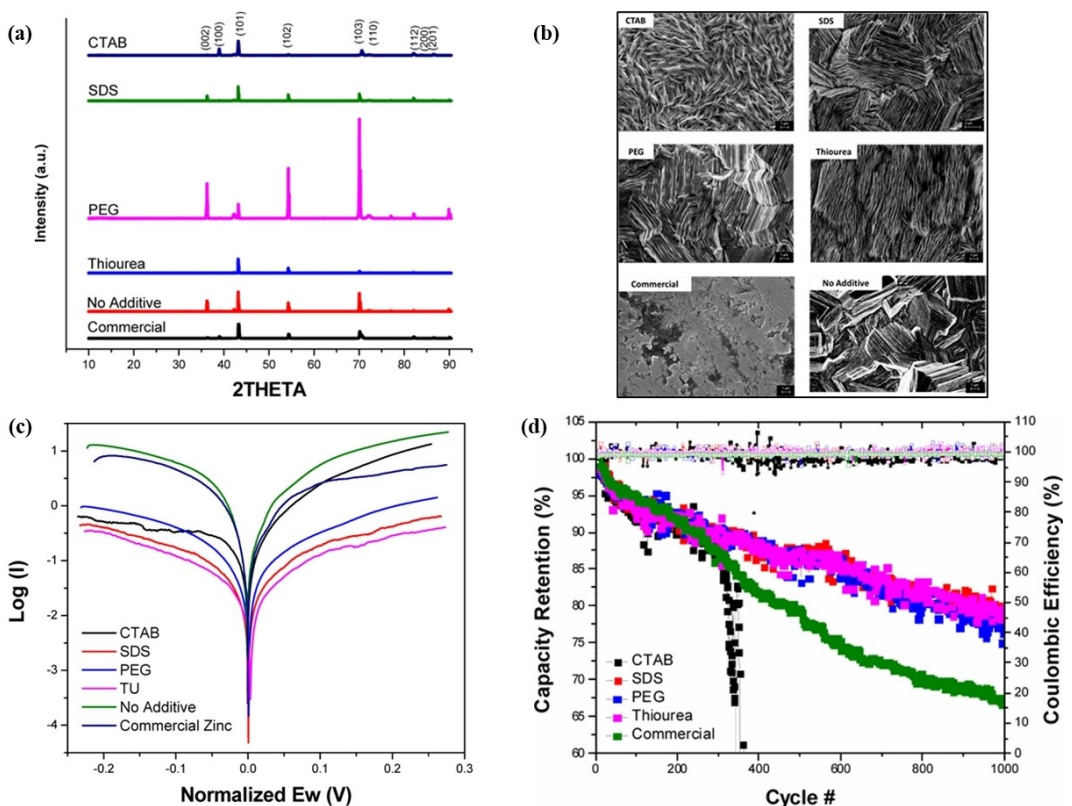


Figure 6. a) XRD results, b) SEM images and c) Linear polarization curves of electroplated zinc anodes. d) Cyclability of the battery with electroplated zinc anodes. Reproduced with permission from Ref. [82]. Copyright (2017) American Chemical Society.

3.1.2. Formation of adsorption film on the anode surface

The additives are inclined to be adsorbed on the zinc electrode surface, forming the adsorption films, and the film-dependent effects are usually associated with localized primary cell reactions that cause metal corrosion on the metal surface. Specific locations on the zinc surface correspond to two types of reactions, that is, anodic reaction and cathodic reaction. Inhibitors of anodic reaction (zinc corrosion) and cathodic reaction (HER) are referred to as anodic inhibitors and cathodic inhibitors, respectively. These film-forming additives facilitate overlay on these reaction sites, through which the zinc corrosion and the reduction of hydrogen ions on the metal surface are hindered.^[85] Furthermore, the side reactions can be controlled by the degree of densification of the anode surface film, in general, the denser it is, the better it is for corrosion inhibition.

Organic additives incorporated into the electrolyte have been demonstrated to be effective in inhibiting the corrosion of zinc electrodes recently. Organic additives can be deposited or adsorbed onto the electrode surface, which seriously affects the electrodeposition of metal ions and the corrosion process of electrodes. Lin et al.^[28] reported the effect of different concentrations of polyethyleneimine (PEI) additives on the corrosion of zinc anode. It is suggested that with increasing PEI concentration, the zinc deposition morphology gradually changes from distinct dendrites to small spherical particles and

finally to a smooth and flat morphology (Figure 8a). It is mainly attributed that PEI changes the orientation of zinc deposition (Figure 8b). The corrosion potential shifts positively and the corrosion current becomes smaller (Figure 8c), indicating that PEI can effectively inhibit the corrosion of zinc anode. Once PEI concentration is up to 50 ppm, the corrosion inhibition rate reaches to 52.2% and zinc anode is smoother. These results can be attributed to the fact that PEI can be adsorbed onto the zinc anode surface during the initial oxidation of zinc, forming a protective layer to avoid direct attack by the alkaline electrolyte. It can slow down the self-corrosion of the zinc anode (Figure 8d). Moreover, the PEI molecular adsorption layer retains the original active sites of the electrode and promotes the diffusive deposition of zinc ions. However, HER on the zinc anode is strong due to the side reactions caused by the PEI, therefore, the concentration of PEI is suggested to be controlled reasonably. In order to explain the corrosion inhibition mechanism more clearly, Banik et al.^[86] found that PEI can inhibit dendrites growth during zinc electrodeposition in alkaline solutions. With the help of PEI, the tip morphologies of the dendrites are changed from a sharp shape to a rounded spherical shape, as shown in Figure 8e. The adsorption of PEI molecules at the tips of dendrites is responsible for hindering the gradual diffusion of Zn^{2+} in the vicinity of dendrites. Therefore, uniform Zn^{2+} deposition can be obtained by suppressing the "tip effect". Uniform zinc deposition leads directly to a smooth zinc deposit layer, which reduces the

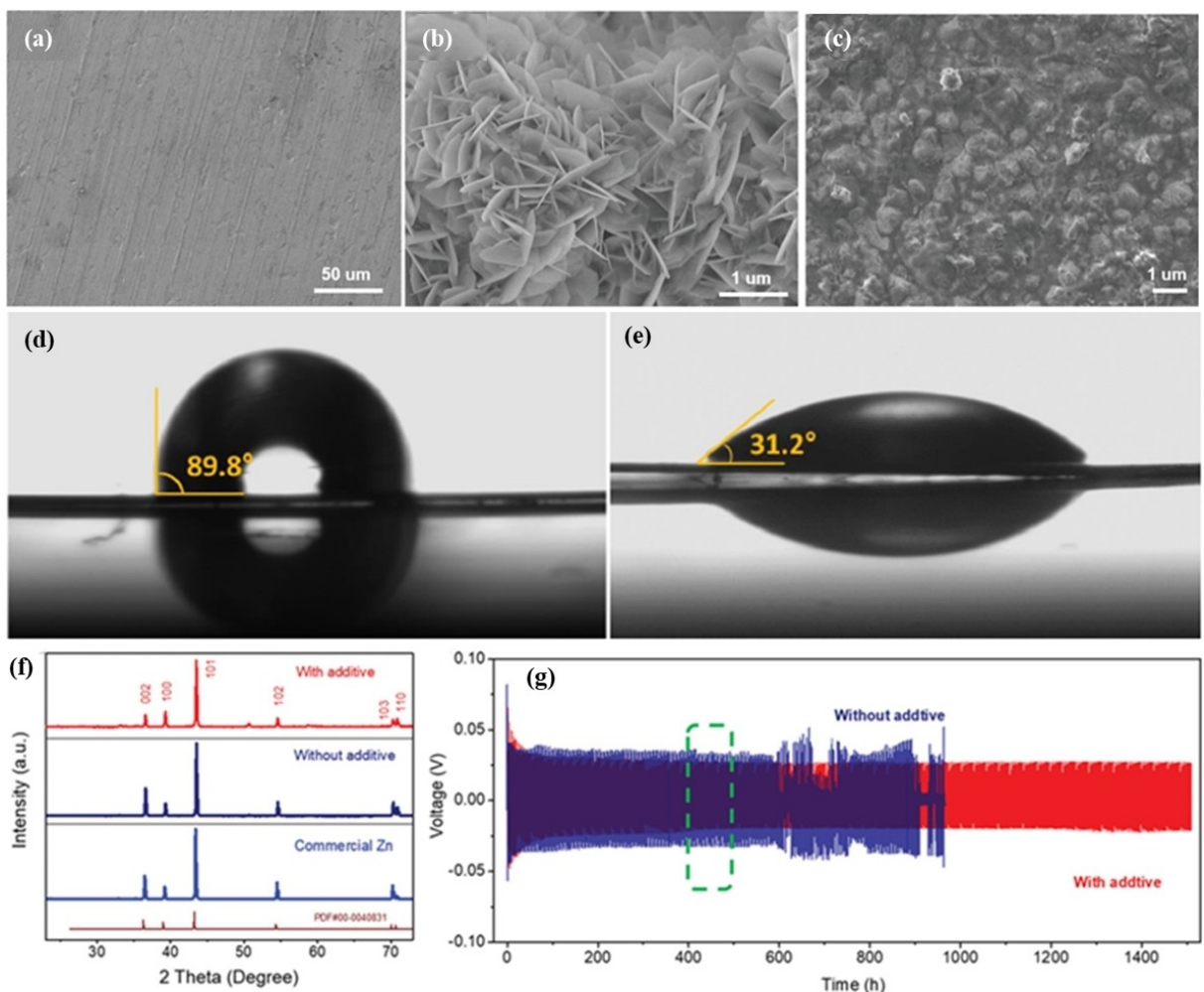


Figure 7. SEM images of a) bare zinc foil, and electrodeposited zinc electrodes b) without SDBS and c) with SDBS. The contact angle between zinc foil interface and electrolyte d) without SDBS and e) with SDBS. f) The effect of SDBS on electrodeposited zinc electrodes. g) Voltage curves of zinc symmetric cells without and with SDBS. Reproduced with permission from Ref. [84]. Copyright (2019) Wiley-VCH.

reactivity of the electrode-electrolyte interface and inhibits the tendency of zinc corrosion.

The PEI mentioned above belongs to surfactants, a class of organic additives considered to be effective additives. Surfactants are structurally composed of two parts: polar groups adsorbing on the zinc surface and non-polar groups escaping from the zinc surface. A protective layer can be formed to prevent direct contact between zinc and water, inhibiting zinc corrosion. The adsorption of additives affects the reactions occurring on the zinc electrode surface. A recent study demonstrates that the addition of tetrabutylammonium sulfate (TBA_2SO_4) limits the corrosion reaction of zinc in the electrolyte.^[87] The competitive adsorption of TBA^+ during charging resulted in the hindrance of Zn^{2+} diffusion to the electrode surface (Figure 9a). The surface adsorption of TBA^+ is further demonstrated by linear polarization experiments, where the corrosion current of the zinc anode is reduced by the addition of TBA_2SO_4 (Figure 9b). In further, sodium dodecyl sulfate (SDS) is an anionic surfactant and widely used as an additive in aqueous battery electrolytes.^[82,88,89] SDS ionizes into

Na^+ and dodecyl sulfate groups in water and the dodecyl sulfate group has a negative charge. A sulfate is a hydrophilic group, and oxygen atoms are adsorbed on the zinc surface instead of zinc atoms. The long hydrophobic alkyl chains reach into the aqueous solution, thus acting as a hydrophobic layer. Hou et al.^[89] added SDS with critical micelle concentration to a 1 M $\text{ZnSO}_4 + 1 \text{ M Na}_2\text{SO}_4$ electrolyte system to investigate the effect of SDS on zinc electrodes. The results show that SDS increases the hydrogen evolution overpotential, decreases the oxygen precipitation overpotential, expands the electrochemical window of the electrolyte and suppresses the occurrence of hydrogen and oxygen precipitation in the electrolyte (Figure 9c). To explain the mechanism of SDS action, the theoretical calculations have confirmed that SDS adsorbed on the zinc anode surface forms a hydrophobic layer, hindering the contact of water with the zinc surface (Figure 9d). It exhibits less possibility to decompose into hydrogen and oxygen as well as expand the electrochemical window of the electrolyte. Furthermore, zinc ions diffuse more easily and with fewer dendrites and by-products. Polyethylene glycol (PEG) is also a commonly

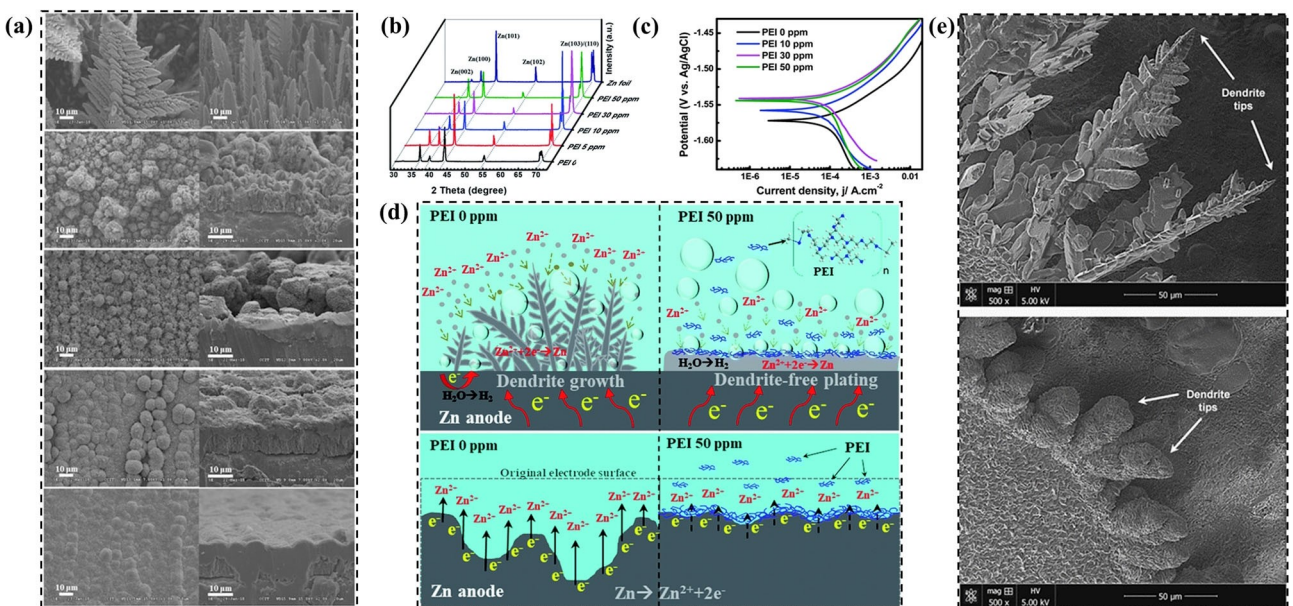


Figure 8. a) SEM images of zinc deposits with various concentrations of PEI. b) XRD patterns and c) Polarization curves of zinc anodes. d) Schematic illustration of the effects of PEI additive on zinc deposition and corrosion. Reproduced with permission from Ref. [28]. Copyright (2020) Royal Society of Chemistry. e) SEM images of zinc dendrites without and with 10 ppm PEI. Reproduced with permission from Ref. [86]. Copyright (2014) Elsevier.

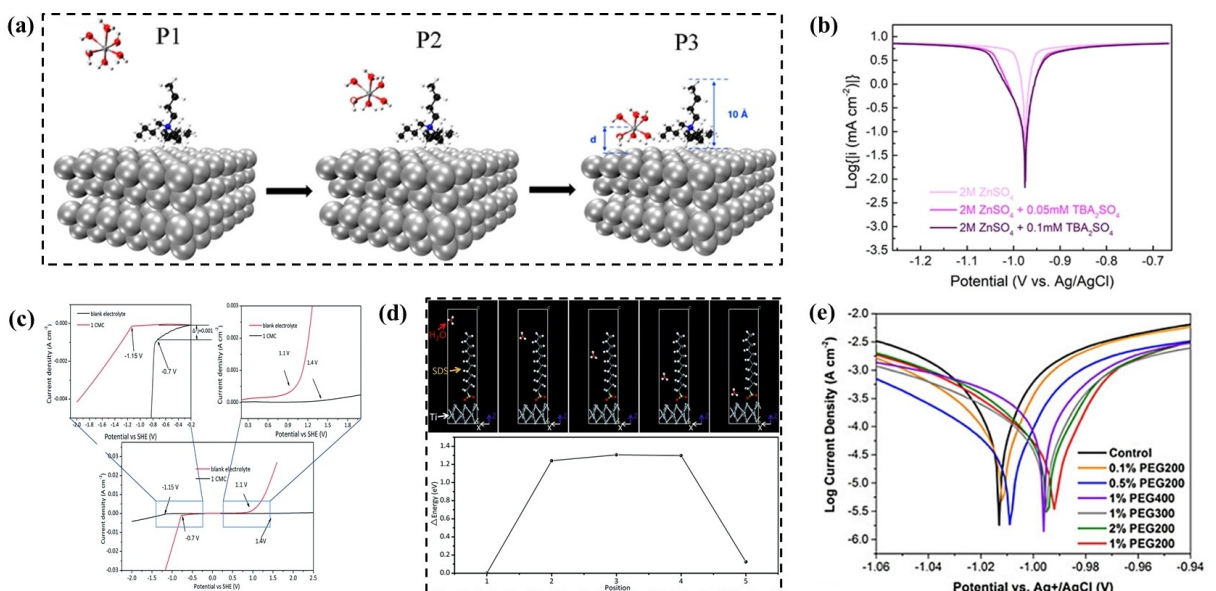


Figure 9. a) Schematic illustration of the interaction of hydrated zinc ions with the adsorption layer. b) Linear polarization curves of zinc anodes in different electrolytes. Reproduced with permission from Ref. [87]. Copyright (2020) American Chemical Society. c) Electrochemical stability windows of different electrolytes by linear sweep voltammetry. d) Diffusion energy barriers of water molecules through different positions of the SDS adsorption layer. Reproduced with permission from Ref. [89]. Copyright (2017) Royal Society of Chemistry. e) Linear polarization plots of zinc anodes with different volume fractions of PEG 200. Reproduced with permission from Ref. [90]. Copyright (2018) Wiley-VCH.

nonionic surfactant, whose molecules contain ether groups as the main hydrophilic groups. Mitha et al.^[90] studied in-depth the effects of PEG 200 as an electrolyte additive on zinc electrodes. It is shown that PEG molecules occupy active adsorption sites on the zinc electrode surface, thus limiting the diffusion of Zn^{2+} from the solution to the surface and inhibiting dendrite growth. At the same time, PEG molecules preferentially occupy nucleation sites on the zinc electrode surface to

prevent the adsorption of H^+ on the zinc anode. Thus, HER and corrosion can be restrained. Linear polarization test results show a significant positive shift in corrosion potential and a low corrosion current density of 0.29 mA cm^{-2} for the zinc electrode in 1 vol% PEG 200 electrolyte, which is lower than that of commercial zinc foil (Figure 9e). Besides, surfactants such as ionomers,^[91] polyoxyethylene alkyl phosphate ester acid form (GAFAC RA600),^[92] polyethyleneglycols (PEG 600, PEG

400),^[92–94] and poly (ethylene glycol) bis (carboxymethyl) ether (PEG DiAcid 600)^[94] have been used as corrosion inhibitors for alkaline zinc-based batteries.

A single additive would be not effective for corrosion inhibition. It has been shown that the synergistic effect of compound additives can greatly inhibit zinc corrosion. Liang et al.^[95] used polyethyleneglycol 600 (PEG 600) and polysorbate 20 (Tween 20) as compound corrosion inhibitors in alkaline zinc batteries to reduce zinc corrosion. It is shown that PEG 600 or Tween 20 could inhibit zinc corrosion to some extent by inhibiting HER (Figure 10a and b). Tween 20 adsorbs more readily to the zinc surface because of its higher polarity compared to PEG 600. Due to the highly branching structure of Tween 20, the zinc surface cannot be completely covered, while linear PEG could cover the remaining active sites (Figure 10c). Similarly, imidazole (IMZ) and polyethylene glycol 600 (PEG 600) have a synergistic effect (Figure 10d). IMZ inhibits zinc corrosion by inhibiting the anodic reaction, while PEG inhibits the cathodic reaction.^[96]

In fact, the essence of corrosion can be described as a miniature primary cell consisting of anodic and cathodic electrochemical reactions occurring on the surface of a metal. Additionally, the crystal surface texture may influence the corrosion due to the difference in crystal surface energy at each location. Effective anodic surface films (e.g., SDS, PEG, and PEI) may cover the metal surface and thus influence the evolution of the texture leading to an inhibitory corrosion reaction. The composite electrolyte additive has a higher surface coverage and exhibits higher corrosion resistance than a single additive.

As above mentioned, HER and zinc corrosion are concomitant reactions. The hydrogen production leads to cell expansion, which eventually causes electrolyte leakage and short-circuiting. Increasing the hydrogen evolution overpotential can inhibit the HER. Lee et al.^[97] investigated the effects of four

organic acid additives on HER and found that all these acids increase the hydrogen evolution overpotential. Among them, tartaric acid has a positive effect (Figure 10e). During cathodic polarization, a negative charge is present on the surface of the ZnO electrode, however, these acids induced an increased hydrogen evolution overpotential of the ZnO electrode. Therefore, the adsorption of these molecules is related to the organic groups in the acid. In addition, quaternary additive mixtures (PEG, CTAB, BA and TU) are also effective in inhibiting HER.^[98] These additives can exhibit the aforementioned properties through blocking at the active center of the zinc surface.

3.1.3. Hydrogen-bonding effect

The root cause of corrosion originates from water in the electrolyte. How to reduce the activity of free water is a point of interest for research. Besides being adsorbed on the zinc anode, some additives with the polar group would create H-bonding with free water. A recent study has shown that H-bonding can be formed between 1,2-dimethoxyethane (DME) containing ether groups and free water.^[99] Figure 11(a) shows that the activity of water is reduced, achieving the inhibition of HER and zinc corrosion. It can be seen from Figure 11(b) that the HER tends to occur in mild acidic electrolytes. With the concentration of DME increasing, the hydrogen precipitation onset potential shows a distinct negative shift from -1.09 to -1.20 V (vs. Ag/AgCl). Figure 11(c) shows more visually that the rate of H_2 precipitation is reduced by the addition of DME additives. Thus, by reducing the activity of water in the electrolyte, DME successfully inhibits HER. In order to visually express the corrosion inhibition efficiency, linear polarization tests are conducted (Figure 11d). The H-bonding between DME and water molecules inhibits the HER caused by excess free

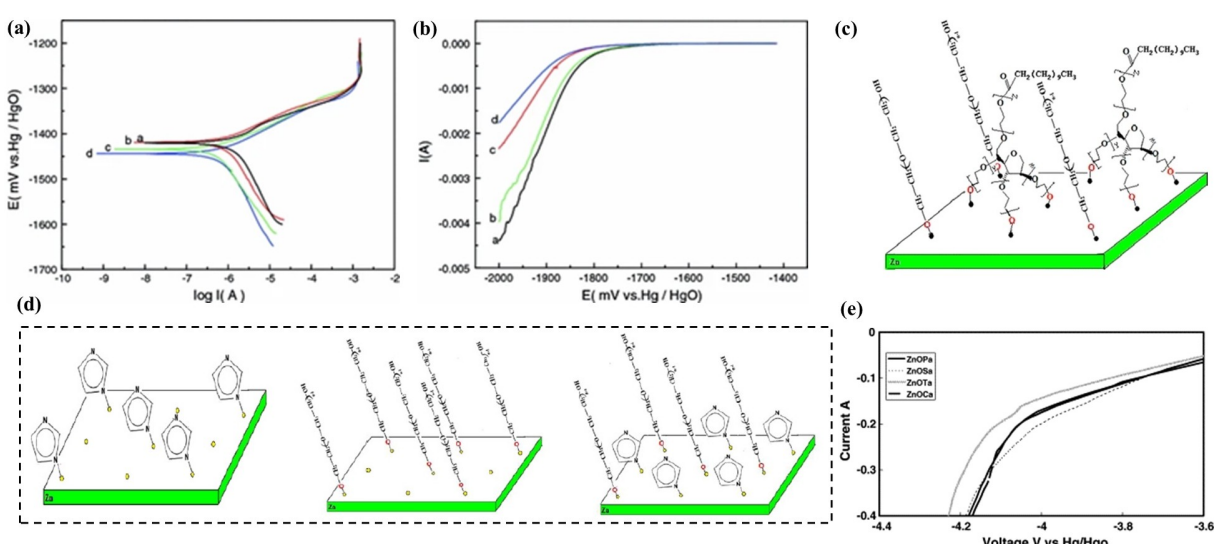


Figure 10. a) Tafel plots and b) Cathodic polarization curves of zinc in 3 M KOH solution. c) Schematic illustration of composite inhibitor adsorption on the zinc surface. Reproduced with permission from Ref. [95]. Copyright (2011) Springer Nature. d) Possible adsorption mechanism of PEG 600, IMZ, and composite additive on the zinc surface. Reproduced with permission from Ref. [96]. Copyright (2011) Elsevier. e) Cathodic polarization curves of the zinc electrodes with different additives. Reproduced with permission from Ref. [97]. Copyright (2005), Elsevier B.V.

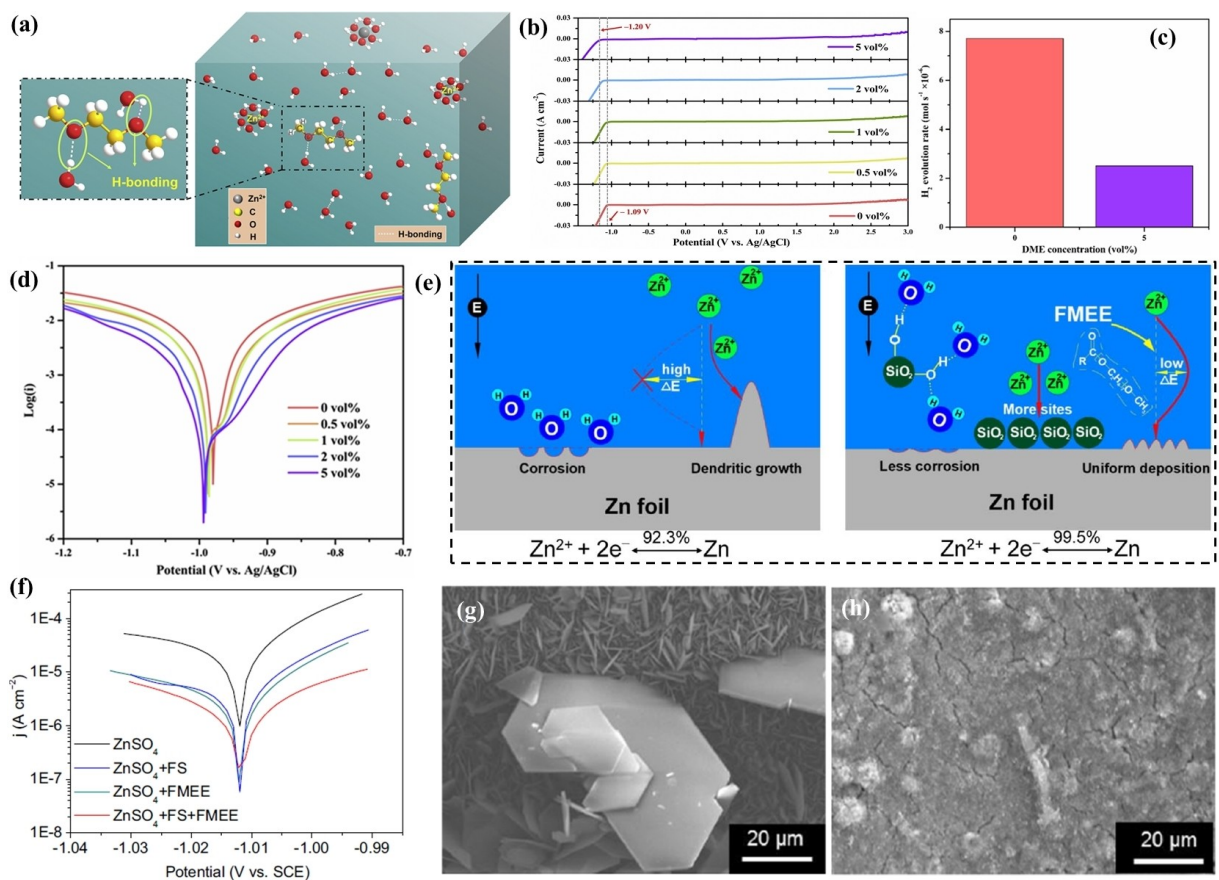


Figure 11. a) An illustration of DME with water molecules forming H-bonding. b) Electrochemical stability windows of various electrolytes. c) H₂ evolution rate in different electrolytes. d) Tafel plots of zinc anodes in different electrolytes. Reproduced with permission from Ref. [99]. Copyright (2020) Elsevier. e) Schematic diagram of zinc stripping/plating processes in different electrolytes. f) Tafel plots of zinc when in contact with different electrolytes. Morphology of Zn metal surface after cycling in g) ZnSO₄ electrolyte and h) ZnSO₄ + FS + FMEE electrolyte. Reproduced with permission from Ref. [100]. Copyright (2019) The Electrochemical Society.

water, and, DME adsorbs on the electrode surface, which is responsible for the reduced corrosion current density of zinc foil in electrolytes containing DME. therefore, the hydrogen precipitation corrosion is hindered to some extent. To reduce the content of free water, Huang et al.^[100] developed a new electrolyte system containing fumed silica (FS) and fatty methyl ester ethoxylate (FMEE). It can immobilize water molecules and control Zn²⁺ deposition, and the FS additive can form hydrogen bonds with free water molecules to inhibit water-induced corrosion. Moreover, as an inorganic filler, FS can enhance the mechanical strength of the diaphragm and prevent the growth of zinc dendrites. The FMEE additive facilitates the uniform dispersion of Zn²⁺ in the aqueous solution and reduces the activation energy of Zn²⁺ deposition. Therefore, Zn dendrites can be hindered (Figure 11e). The reduction of the corrosion current density and the decrease of the corrosion products of zinc anode can be seen from the Tafel plots and the SEM images after cycling (Figures 11f-h).

3.1.4. Effects of the solvation shell

Typically, a zinc ion is surrounded by six water molecules to form a solvation shell, which is mainly responsible for zinc corrosion and hydrogen precipitation. Sun et al.^[101] attempted to use glucose to modulate the solvation environment of zinc ions, which successfully improved the plating/stripping processes of zinc anodes. It is shown that one glucose molecule could replace one water molecule in the initial solvated shell of Zn²⁺, which effectively prevents severe side reactions on the surface of the zinc anode. At the same time, glucose molecules prefer to be adsorbed on the zinc metal surface, promoting the transfer of Zn²⁺ and changing the electric field distribution (Figure 12a). The SEM images of zinc anode after deposition in zinc symmetric cell show no obvious corrosion by-product with the addition of glucose (Figure 12b). The corrosion current density of zinc foil in ZnSO₄-glucose electrolyte is lower than that in pure ZnSO₄ electrolyte, indicating that glucose helps to avoid the formation of by-products (Figure 12c), which is consistent with the results of XRD patterns (Figure 12d). Furthermore, dimethyl sulfoxide (DMSO) has also been reported to contribute to side reactions inhibition.^[102] The typical Zn²⁺ solvation sheath [Zn(H₂O)₆]²⁺ will be regulated to

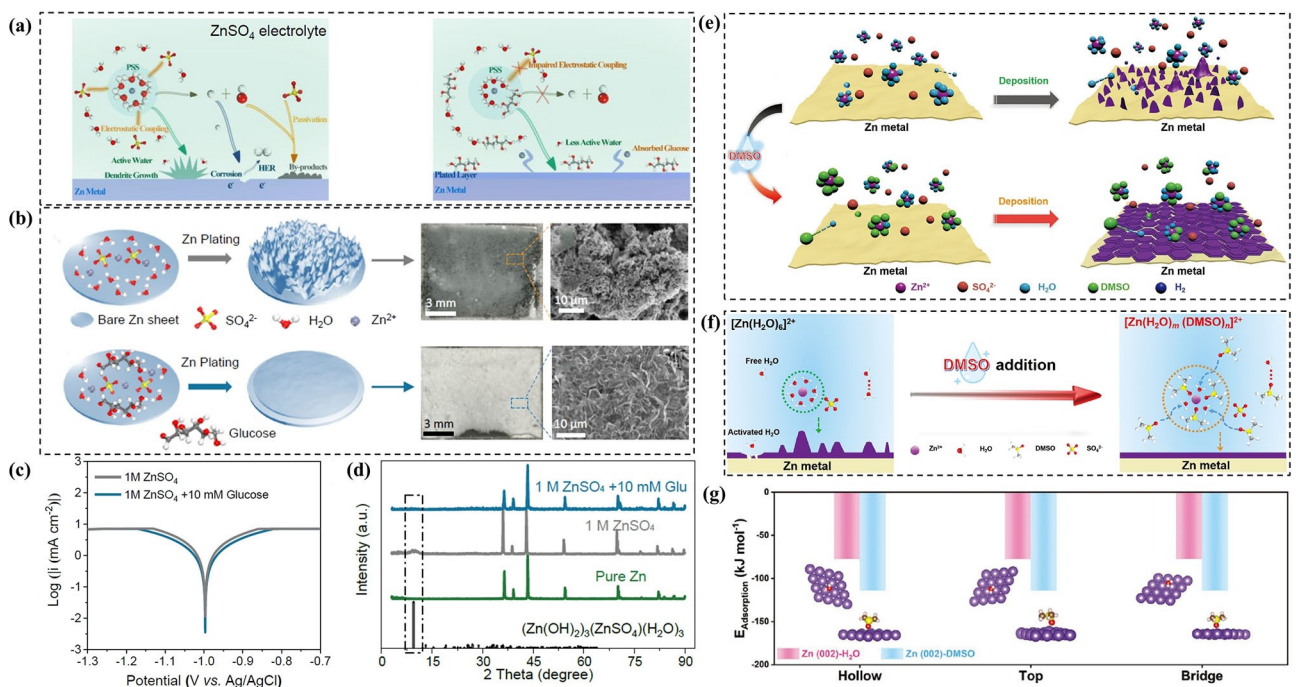


Figure 12. a) Schematic illustration of different reaction processes occurring on the zinc anode surface. b) Scheme of zinc plating processes in different electrolytes and corresponding SEM images after deposition. c) Tafel plots of Zn foil under ZnSO₄ and ZnSO₄-glucose electrolytes. d) XRD patterns of zinc anodes after 100 h cycles under various electrolytes. Reproduced with permission from Ref. [101]. Copyright (2021) Wiley-VCH. e) Schematic illustration of zinc deposition behaviors in different electrolytes. f) Conceptual diagrams of the Zn²⁺ solvation structures in reference electrolyte and hydrogen bonds evolution in DMSO hybrid electrolytes. g) Binding energy of Zn (002) plane with H₂O and DMSO. Reproduced with permission from Ref. [102]. Copyright (2021) Wiley-VCH.

immunize the side reactions because DMSO has higher binding energy for Zn²⁺ due to the reconstruction of stronger S=O·H–O hydrogen bonds affecting higher adsorption energy to zinc (002) plane, which will guide zinc deposition to form (002) texture without zinc corrosion (Figures 12e–g). Other desolvantizing has similar corrosion inhibition mechanisms, that is, the introduced additive molecules replace certain H₂O molecules in the primary solvated shell, reducing the undesirable reactions involving free water and possibly directing the meritocratic orientation of the zinc grains.

3.2. Zinc alloying

The design of different types of zinc alloys has become a proven strategy to inhibit HER and zinc corrosion.^[50,103–111] Compared to pure zinc, the formation of intermetallic phases leads to higher chemical bonding strength between phases, denser arrangement of atoms and lower Gibbs free energy (Figure 13). It increases the hydrogen precipitation overpotential and causes a positive shift in corrosion potential with a decrease in corrosion current density.^[50,105,111–113] The Tafel relationship between the hydrogen evolution overpotential and the current density of the metal is as follows [Equation (14)].

$$\eta = a + b \log i \quad (14)$$

where a , b indicates the overpotential value per unit current density and the Tafel slope, respectively. Generally, the b value of metals does not vary much. The a value varies a lot, mainly related to the material itself and the solution. These metal elements generally exhibit high hydrogen precipitation overpotential and corrosion resistance, such as Fe, In, Co, Ni, Sn, Pb, Sb, Bi, Cu and Hg,^[43] and the a value of these metals are generally greater than 0.5 V, as shown in Table 1.

Studies have shown that zinc undergoes uneven chemical corrosion in a mild acidic solution, such as ZnSO₄ solution. The product Zn₄(OH)₆SO₄·5H₂O adheres to the zinc surface, forming an uneven, porous film and releasing H₂.^[50] The porous film would not isolate electrolytes, causing continuous corrosion (Figure 14a). To suppress this phenomenon, Cai et al.^[50] prepared Cu/Zn electrodes by soaking zinc in an ethanol solution containing 0.1 M CuCl₂ with heat treatment (Figure 14b). The Cu–Zn alloy not only leads to stable deposition of metallic zinc without dendrites formation, but the Cu–Zn/Zn compound electrode has a lower corrosion rate compared to pure zinc (7.94 μAcm⁻² vs. 37.15 μAcm⁻²) (Figure 14c). It is shown that the reduced corrosion rate is related to the generation of Cu₅Zn₈ intermetallic compounds on the Cu–Zn alloy surface. The formation of corrosion-resistant intermetallic compounds hinders the harmful contact of the alloy with the electrolyte (Figure 14d). Cycling testing of the symmetric cell shows a long cycle life of 1500 h at a low current density, further demonstrating the improved electrochemical performance (Figure 14e). Cu is widely used in alloying studies due to

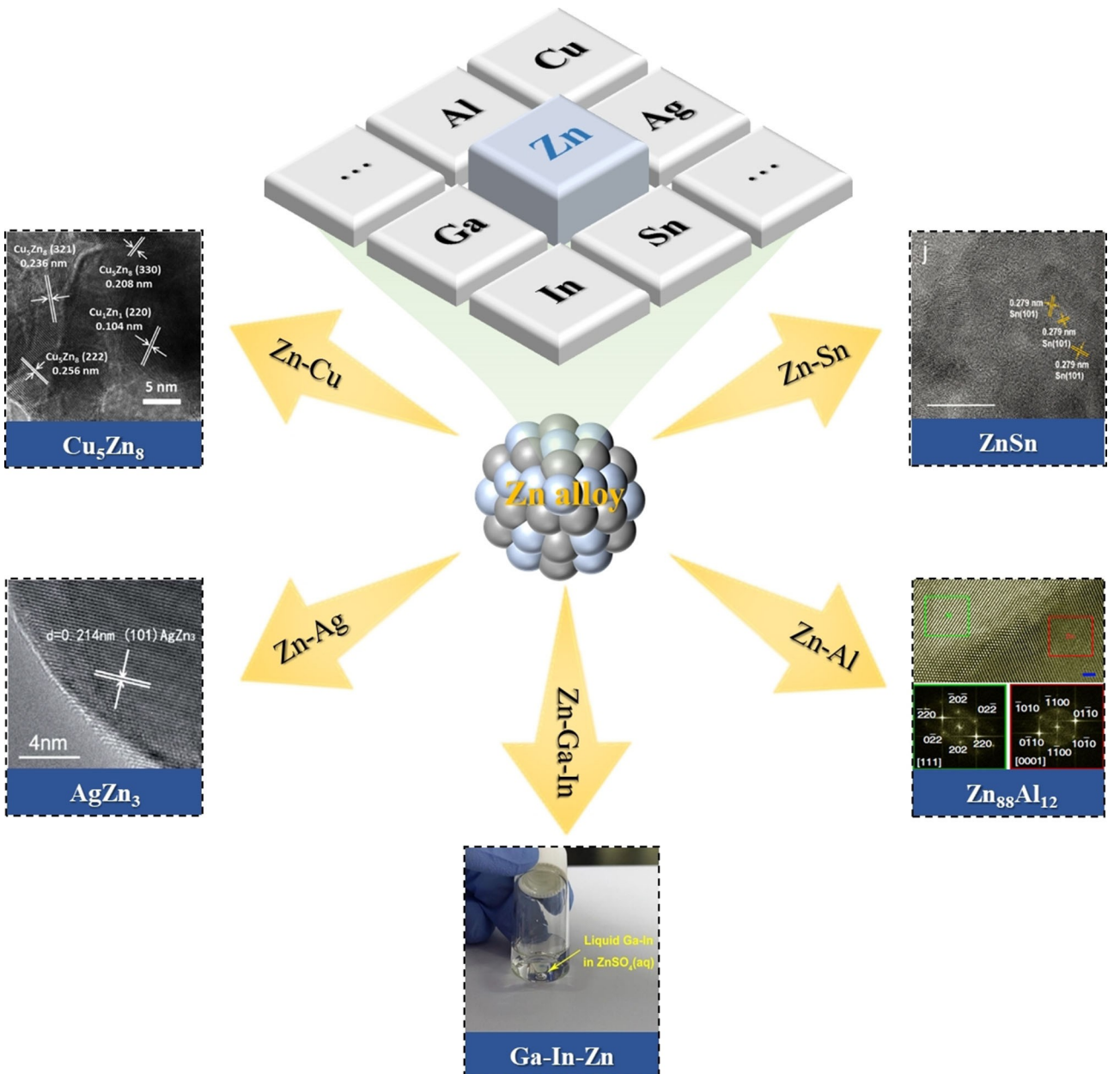


Figure 13. Reported zinc alloying and their possible contributing phases for zinc anodes.

the high redox potential (0.34 V vs. SHE), low cost, good electrical conductivity, structural stability, and compatibility with zinc. In addition to Cu elements, other metallic elements are gradually applied in alloying studies. Han et al.^[103] proposed an effective strategy to decorate the zinc surface with a bifunctional metal In layer to suppress drastic corrosion. Corrosion is serious on zinc anodes in aqueous ZnSO₄ electrolytes during battery rest and cycling processes (Figure 14f). After 8 days of standing in an aqueous ZnSO₄ electrolyte, a typical corrosion product, hexagonal flakes of different sizes, can be observed on zinc surface, while the Zn|In foil retains its original morphology, as shown by XRD analysis confirming this phenomenon (Figure 14g and h). For the bare Zn symmetric cell after cycling, a 62% significant thickness increase can be

observed in Figure 14(i). In contrast, no gas escape can be detected on the Zn|In surface. By comparing the onset potential for the hydrogen evolution reaction on Zn|In foil and bare Zn foil, it can be found that In inhibits the release of HER, which is demonstrated by linear scanning voltammetry curves (Figure 14j). All the above results show that the In acts as a favorable corrosion inhibitor because of its good chemical inertness (−0.338 V vs. SHE) and high hydrogen evolution overpotential. Zinc alloys with excellent physicochemical stability obtained by different preparation processes have a positive impact on corrosion inhibition, which makes zinc alloys a possible focus of subsequent research.

Table 1. Values of constants *a* and *b* for the cathodic precipitation of hydrogen on some metal surfaces at $(20 \pm 2)^\circ\text{C}$ (V).

Metals	Acidic solution		Alkaline solution	
	<i>a</i>	<i>b</i>	<i>a</i>	<i>b</i>
Ag	0.95	0.10	0.73	0.12
Al	1.00	0.10	0.64	0.14
Au	0.40	0.12	—	—
Be	1.03	0.12	—	—
Bi	0.84	0.12	—	—
Cd	1.40	0.12	1.05	0.16
Co	0.62	0.14	0.60	0.14
Cu	0.87	0.12	0.96	0.12
Fe	0.70	0.12	0.76	0.11
Ge	0.97	0.12	—	—
Hg	1.41	0.114	1.54	0.11
Mn	0.80	0.10	0.90	0.12
Mo	0.66	0.08	0.67	0.14
Nb	0.80	0.10	—	—
Ni	0.63	0.11	0.65	0.10
Pb	1.56	0.11	1.36	0.25
Pd	0.24	0.03	0.53	0.13
Pt	0.10	0.03	0.31	0.10
Sb	1.00	0.11	—	—
Sn	1.20	0.13	1.28	0.23
Ti	0.82	0.14	0.83	0.14
Tl	1.55	0.14	—	—
W	0.43	0.10	—	—
Zn	1.24	0.12	1.20	0.12

3.3. Electrodeposited Zn

Several problems are posed when using commercial zinc flakes or zinc foils as the anode, such as the rough surface, the corrosion and the decreased utilization of the pristine zinc.^[114–116] The electrodeposition morphology of Zn anode is related to the binding energies between various collectors and Zn (Figure 15a and b). Copper-based materials are the suitable substrates for Zn electrodeposition due to their lower nucleation overpotential and high binding energies than other substances.^[117,118] The corrosion of the bare Zn electrode edges gradually occurs from the outside to the inside. Fortunately, the volumetric integrity of the Zn electrode is determined by the stable physicochemical properties of copper in aqueous solutions after cycling (Figure 15c). In addition, it has also been reported that zinc alloying by electrodeposition can suppress side reactions.^[112,119] It is regarded that the larger value of the Gibbs free energy change of H adsorption (ΔG_{H}^*) is, the lower possibility of the HER occurrence is.^[112] For example, the doping of Sn atoms could enlarge the ΔG_{H}^* of hydrogen adsorption sites in Zn–Sn alloy, inhibiting HER (Figure 15d). Therefore, the electrodeposited Zn with other doped metals would be a promising candidate for RAZMBs.

3.4. Coating treatments

3.4.1. Inorganic and organic coatings

Apart from the electrolyte additives and zinc alloying strategies described above, coating technology is also a good means of corrosion protection. Several advanced coating materials have

been developed to regulate the electrochemical environment of zinc anode surface and provide physical protection to the interfacial layer. Thus, the effective coating can act as a multifunctional layer that protects or regulates the chemical/electrochemical properties and processes at the interface.^[120] Commonly used coatings can be classified as inorganic and organic, where inorganic coatings are mainly carbon-based materials and metal oxides (e.g., graphite, CaCO_3 , TiO_2 , ZrO_2 , etc.),^[44,121–125] and organic coatings are mainly some polymers (e.g., PVB, 502 glue, Gel-MA, etc.).^[45,46,126–130]

The construction of an insulating nano protective layer on the surface of zinc foil by in situ or non-in situ methods is beneficial to mitigate zinc corrosion. For example, Zhao et al.^[125] deposited the TiO_2 layer on the zinc anode surface (Figure 16a). The corrosion curves show that the corrosion current density of the modified zinc anode is reduced, and the self-discharge test shows that no electrolyte leakage due to hydrogen precipitation occurred in the $\text{Zn}-\text{MnO}_2$ cell with TiO_2 -modified zinc anode (Figure 16b and c). Direct contact of zinc in the electrolyte is avoided effectively by the TiO_2 coating layer, thus inhibiting hydrogen evolution from the anode surface during zinc deposition and reducing zinc corrosion. Existing research studies have shown that Maxwell-Wagner polarization is favorable for uniform zinc deposition and corrosion inhibition. Liang et al.^[124] prepared highly reversible zinc anodes via coating ZrO_2 nanoparticles on the zinc surface (Figure 16d). ZrO_2 coating layer act as an inert property that could prevent zinc corrosion thanks to the high dielectric constant and good chemical stability of ZrO_2 in aqueous electrolytes (Figure 16e). Moreover, the morphology of the zinc electrode is still smooth after cycling (Figure 16f). Thus, on account from Maxwell-Wagner polarization effect of the ZrO_2 , improved electrochemical performance is obtained. Similarly, modification of zinc surface with kaolin (KL) with porous structure and selective permeability to specific elements limits the aggregated deposition of Zn^{2+} , whose inherent physical inertness makes it a natural barrier layer, and the linear polarization curves confirm the reduction of corrosion current (Figure 16g and h).^[123] Carbon-based materials have also been used as coatings for optimizing zinc anode due to good electrical conductivity and chemical stability. Li et al.^[44] prevented the formation of self-corrosion by-products via drawing a graphite layer on the zinc surface using a simple pencil drawing method. The severe corrosion of the pristine zinc foil is shown after 15 days of immersion in 2 M ZnSO_4 solution (Figure 16i), instead, the optimized zinc foil shows no significant color and surface condition changes. Moreover, the edges of the pristine zinc foil at 20–40 min of deposition are locally corroded, while this is not the case for the graphite-covered zinc foil. Hence, graphite gives satisfactory corrosion resistance to zinc anode (Figure 16j and k). Conductive carbon black has similar efficacy.^[131] Self-discharge tests confirmed that the voltage after the shelving of $\text{Zn}-\text{MnO}_2$ batteries with carbon black-coated zinc is about 0.2 V higher than that of batteries with zinc foil, and the result shows that the carbon black coating could inhibit zinc corrosion (Figure 16l–n).

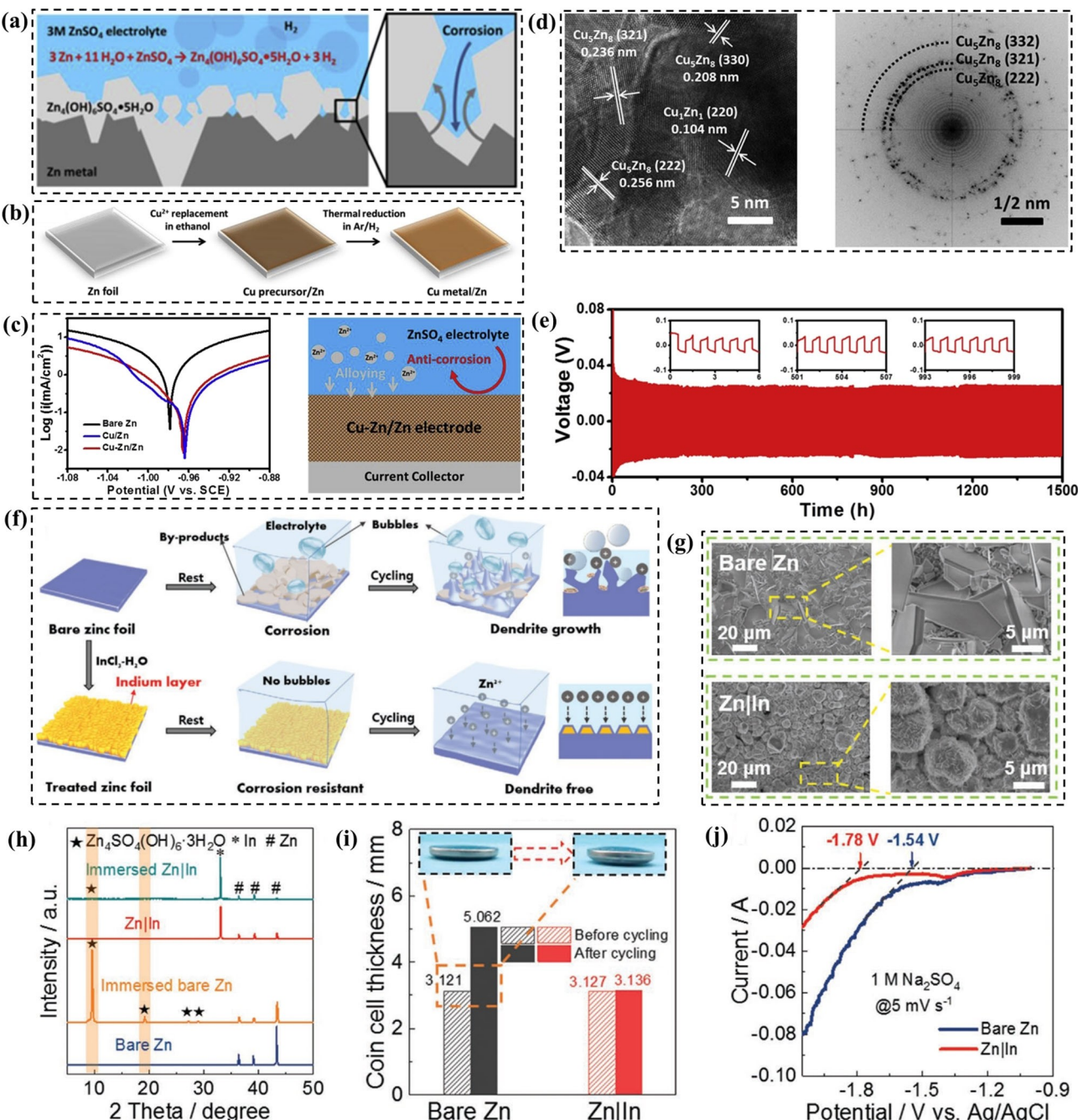


Figure 14. a) Chemical corrosion process of zinc in ZnSO_4 electrolyte. b) Schematic illustration of the Cu/Zn electrode fabrication process. c) Tafel polarization curves of Cu/Zn and Cu-Zn/Zn electrode (left), and the uniform deposition of zinc ions on the Cu-Zn/Zn electrode (right). d) HRTEM image (left), and SAED pattern (right) confirm the existence of intermetallic compounds. e) Cycling stability of Cu/Zn-30d | Cu/Zn-30d symmetric cell. Reproduced with permission from Ref. [50]. Copyright (2020) Elsevier. f) Schematics and characterization of Zn and Zn|In foils. g) SEM images and h) XRD patterns of bare Zn and Zn|In after immersion in 2 M ZnSO_4 electrolyte for 8 days. i) Comparison of the thickness of bare Zn and Zn|In symmetric cells before and after cycling. j) Linear sweep voltammetry curves of bare Zn and Zn|In. Reproduced with permission from Ref. [103]. Copyright (2020) Wiley-VCH.

Organic coatings are generally considered to have the advantages of strong adhesion, flexibility, high ionic conductivity, and good hydrophilicity. Hao et al.^[45] employed a simple spin-coating strategy to uniformly deposit a polyvinyl butyral (PVB) film with high viscoelasticity on the zinc surface. Figure 17(a) shows that after 7 days of immersion in the ZnSO_4 electrolyte, PVB@Zn presents a bright surface without exhibiting corrosion behavior compared to the bare zinc foil. More-

over, only a few corrosion products are visible on the PVB@Zn surface after several tens of cycles, in contrast to the bare zinc foil which shows many by-products on its surface (Figure 17b and c). The strong adhesion on the zinc surface and hydrophilicity of this artificial PVB layer comes from its rich content of oxygen-containing functional groups. Similarly, Park et al.^[127] found that the (3-aminopropyl) triethoxysilane (APTES) can improve the interfacial wettability by forming a special covalent

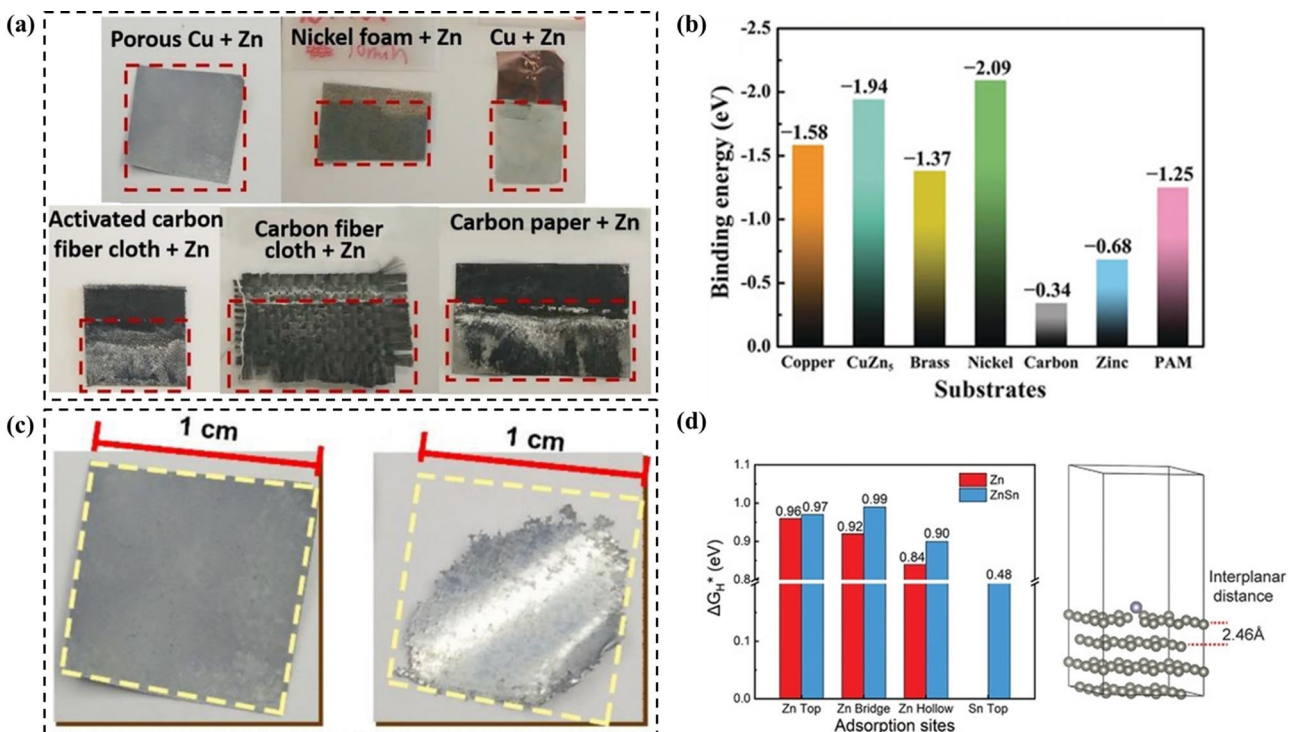


Figure 15. a) Electrodeposition morphology of Zn on different collectors. b) Binding energy of a zinc atom with different substrates. Reproduced with permission from Ref. [117]. Copyright (2019) Wiley-VCH. c) Digital photos of electrodeposition Zn anode and Zn foil after cycling. Reproduced with permission from Ref. [118]. Copyright (2019) American Chemical Society. d) The ΔG_H^* of an H atom adsorbed at selected sites of 4×4 Zn (001) and Zn–Sn (001). Reproduced with permission from Ref. [112]. Copyright (2021) Wiley-VCH.

bond on the metal surface. Therefore, APTES can be coated on the surface of zinc foil to effectively protect zinc metal anodes from corrosive electrolytes. Digital images and SEM images confirm that the layer covers the zinc surface intact (Figure 17d and e). Due to its good hydrophilicity, the contact angle is reduced from the original 81.5° to 13.9° (Figure 17f and g). During the zinc ion stripping/plating process, the rich network of polar bonds present in the 502 glue coating can effectively trap the solvanted water, which can greatly inhibit the occurrence of side reactions (Figure 17h).^[46] Also, the ionic liquid (IL) skinny gel has been reported to be used as a new organic protective layer for zinc anodes.^[128] The unique hydrophobic structure of IL skinny gel repels bulk water molecules from the coating, eliminating interfacial side reactions (Figure 17i). In particular, Jiao et al.^[129] designed a new ion-selective polymer gel (PG) capable of achieving an ultrahigh zinc utilization of 90%, which can be attributed to the simultaneous inhibition of the spontaneous parasitic reaction of zinc with the aqueous electrolyte (Figure 17j). The above results indicate that the layer can effectively inhibit zinc corrosion and HER. Moreover, polyamide (PA) has also been applied to suppress interfacial side reactions resulting from their unique hydrogen bonding network and strong coordination ability with metal ions (Figure 17k).^[132] The surface morphology of different Zn electrodes is clearly shown before and after cycling in Figure 17(l-o). Obviously, the surface of Zn anode is smooth under the protection of PA, indicating the inhibition of HER and corrosion. As an external barrier layer, the coatings, such as

PVB, PG, PA, etc. could adapt to the drastic volume changes occurring on the zinc anode during long-term cycling. Therefore, it is urgently required to develop dynamic adaptive coatings based on organic polymers with high flexibility and ionic conductivity to serve the actual working conditions.

3.4.2. Artificial SEI layers

The coatings constructed by the non-in-situ techniques are usually uneven and not dense, which ineffectively blocks the direct contact between zinc and electrolyte. The coating would be damaged and eventually peeled off during the interfacial fluctuations, leaving an exposed electrode surface in the electrolyte. Thus, the side reactions, including zinc corrosion and hydrogen precipitation, can still occur when the exposed zinc contacts the electrolyte. An artificial solid-electrolyte interphase (SEI) layer with decent adhesion is able to adapt to the interfacial dynamics during cycling. Therefore, the appropriate elements (such as oxygen, sulfur, phosphorus and fluorine element) are introduced to form a robust artificial SEI layer due to the strong chemical bonding force with the Zn atoms together with the high stability in aqueous solution. Compared to the pristine Zn, the ZnF₂ layer can effectively prevent the contact between fresh Zn surface and H₂O molecules, avoiding the interfacial side reactions in the bulk electrolyte, as shown in Figure 18(a and b).^[133] The F atoms are tightly bound with Zn atoms by electrovalent bonds on

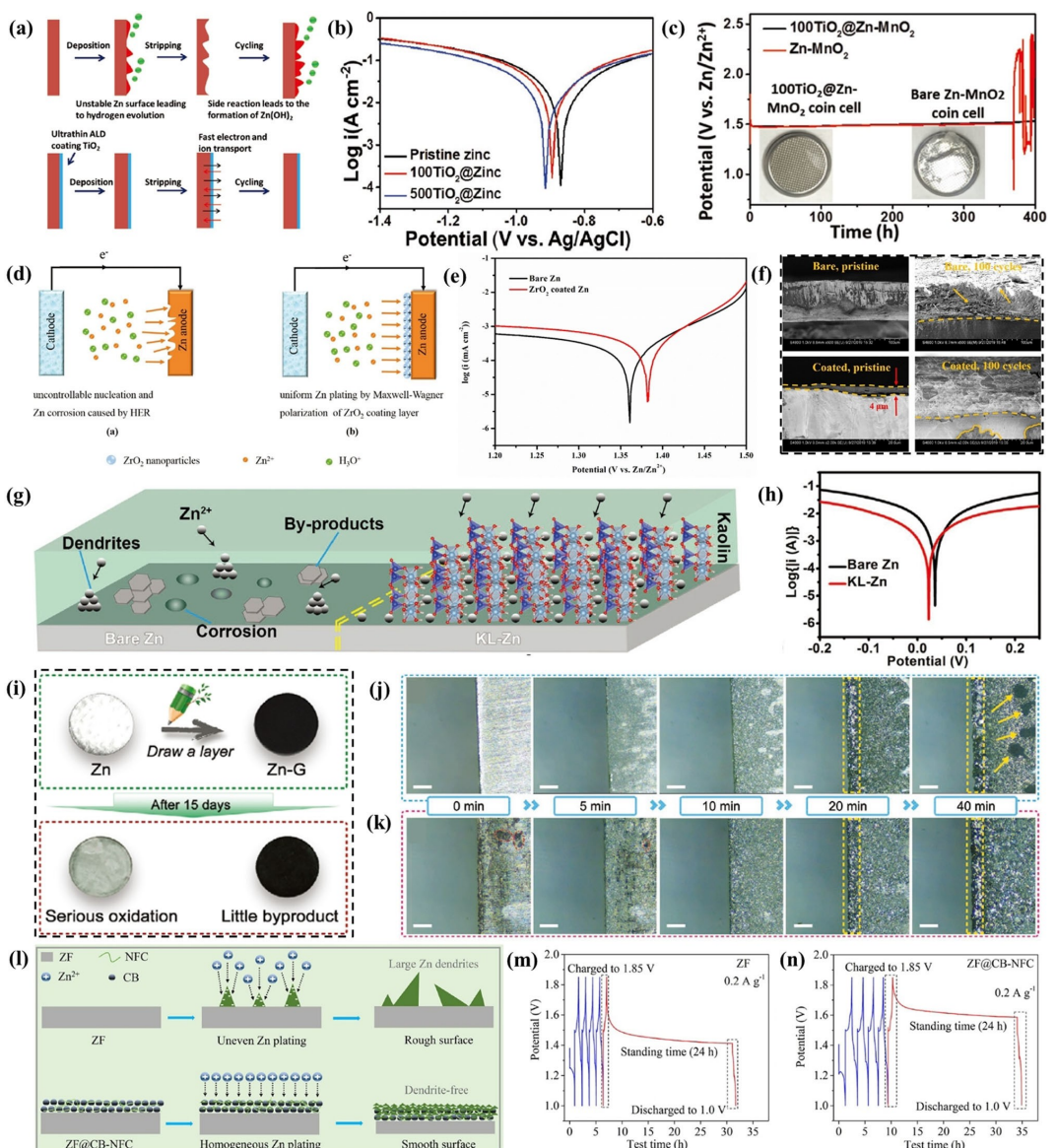


Figure 16. a) A schematic illustration of TiO_2 @Zn. b) Tafel plots of different zinc anodes. c) Self-discharge test of the full cells. Reproduced with permission from Ref. [125]. Copyright (2018) Wiley-VCH. d) Schematic of the stripping/plating processes of the bare Zn anode and the ZrO_2 -coated Zn anode. e) Polarization curves of the bare Zn and the ZrO_2 -coated Zn. f) The typical cross-sectional SEM images of the bare Zn anode and the ZrO_2 coated Zn anode before and after cycling. Reproduced with permission from Ref. [124]. Copyright (2020) Wiley-VCH. g) Interfacial reactions occurring on the Zn and KL-Zn anode surfaces. h) Tafel plots of the bare Zn and KL-Zn. Reproduced with permission from Ref. [123]. Copyright (2020) Wiley-VCH. i) Schematic illustration of the modification process and digital image after immersion in 2 M ZnSO_4 electrolyte for 15 days of Zn and Zn-G anodes. In situ optical microscope photos of j) Zn and k) Zn-G electrodes under various deposition times. Reproduced with permission from Ref. [44]. Copyright (2020) Wiley-VCH. l) Schematic illustrations of the Zn^{2+} deposition processes on the surface of ZF and ZF@CB-NFC anodes. Voltage curves of the self-discharge of the Zn-MnO₂ batteries with m) ZF anode and n) ZF@CB-NFC anode. Reproduced with permission from Ref. [131]. Copyright (2020) Elsevier.

account of the charge migration and redistribution between Zn and F atoms. Similarly, the artificial ZnS layer retains its original protective properties without peeling off even after several repeated folding (Figure 18c).^[134] Moreover, the complex artificial SEI layers with the addition of the special elements, such as $\text{Zn}_3(\text{PO}_4)_2/\text{ZnF}_2$ -rich and $\text{Zn}_3(\text{PO}_4)_2-\text{ZnF}_2-\text{ZnS}$ composite layers, have also been used to modulate interfacial reactions (Figure 18d and e).^[135,136] The unique chemical inertness and high binding power of artificial SEI layers offer a practical possibility to build stable interfaces, and the strategy can be used to exploit the commercial zinc foils with inherent surface defects.

4. Conclusions and Perspectives

In this review, the corrosion behavior of zinc is elucidated in aqueous solutions. Thermodynamically, zinc is unstable and HER inevitably occurs on its surface, producing corrosion products. In alkaline media, ZnO is the main corrosion product that could cover the zinc surface to prevent further corrosion of zinc, but in mild acidic media, the corrosion process is intensified by the corrosion products due to their loose and porous structure. To inhibit zinc corrosion, strategies have been devoted. One is introducing electrolyte additives. The additives

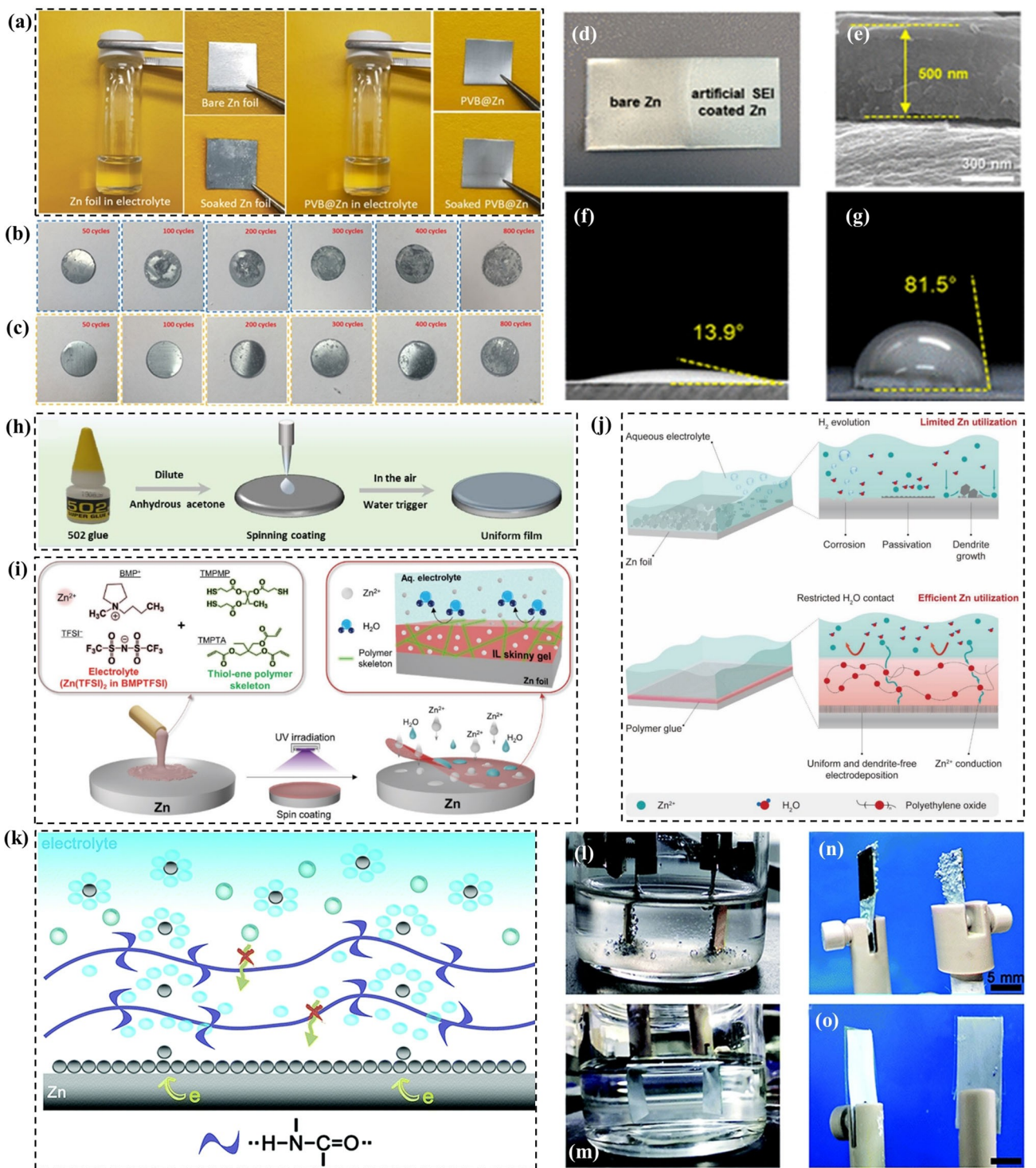


Figure 17. a) Digital images of the bare Zn foil and PVB@Zn foil after soaking in 1 M ZnSO_4 electrolyte for 7 days. b) Zn electrodes and c) PVB@Zn electrodes after cycling. Reproduced with permission from Ref. [45]. Copyright (2020) Wiley-VCH. d) Photograph of the layer coated on Zn foil. e) Cross-sectional SEM image of A-Zn. f) Contact angles of f) A-Zn and g) bare-Zn with 2 M ZnSO_4 electrolyte. Reproduced with permission from Ref. [127]. Copyright (2021) American Chemical Society. h) Schematic diagram of the preparation of a 502 glue protective layer. Reproduced with permission from Ref. [46]. Copyright (2020) Elsevier. i) An illustration of the fabrication of an IL skinny gel on the Zn anode surface. Reproduced with permission from Ref. [128]. Copyright (2021) Wiley-VCH. j) A schematic illustration of zinc plating on the Zn-PG. Reproduced with permission from Ref. [129]. Copyright (2021) Wiley-VCH. k) Schematic diagrams for Zn deposition on the modified Zn. Digital photos of HER for symmetrical Zn cells with l) bare Zn and m) PA-coated Zn. The surface morphology of n) bare Zn and o) PA-coated Zn after cycling. Reproduced with permission from Ref. [132]. Copyright (2019) Royal Society of Chemistry.

can be adsorbed onto the zinc surface to change zinc surface energy. Due to this, zinc would be deposited on an anti-

corrosion texture, such as the (002) plane. Certain additives can also form hydrogen bonds with free water to avoid water

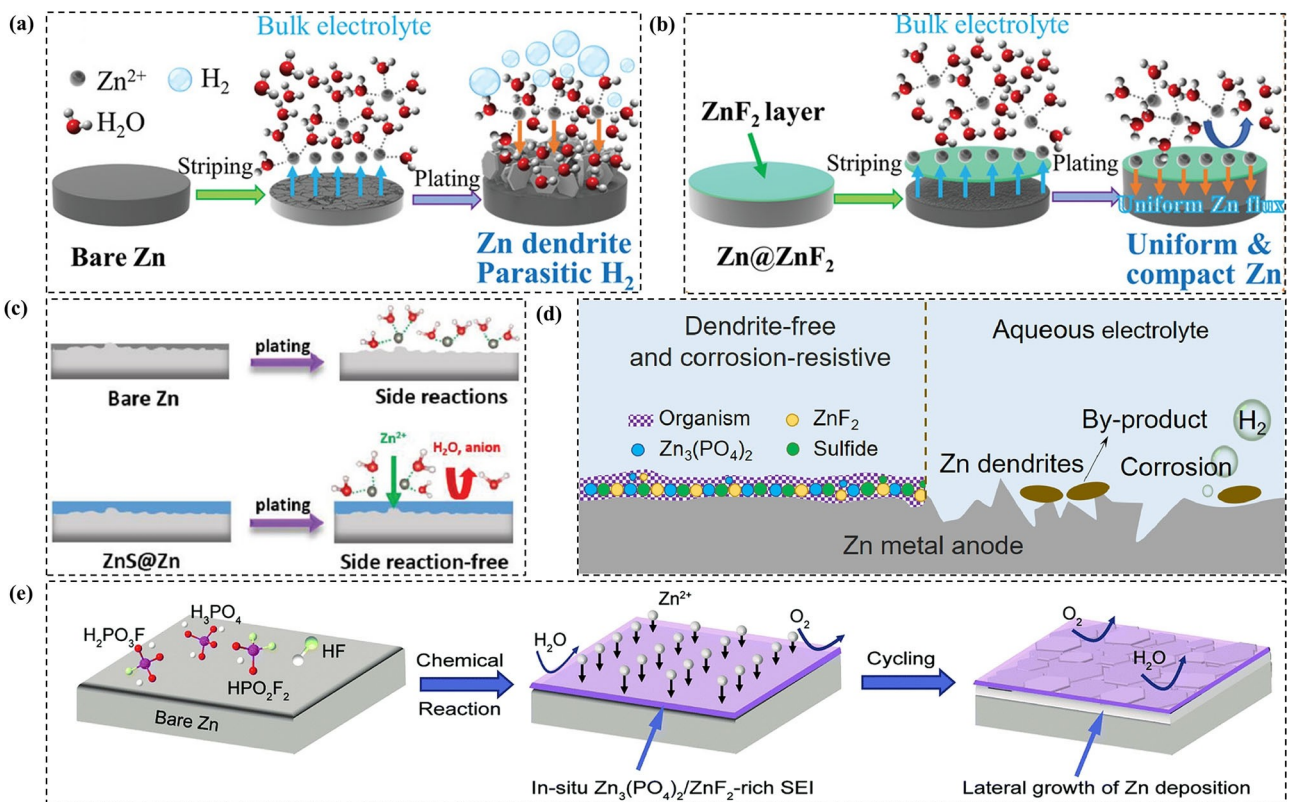


Figure 18. Illustrations of the Zn deposition processes on a) bare Zn foil and b) Zn@ZnF₂ foil. Reproduced with permission from Ref. [133]. Copyright (2021) Wiley-VCH. c) Schematic diagrams of the surface chemistry on bare Zn foil and ZnS@Zn foil. Reproduced with permission from Ref. [134]. Copyright (2020) Wiley-VCH. d) The interface reactions on bare Zn and modified Zn electrodes. Reproduced with permission from Ref. [136]. Copyright (2021) Elsevier. e) Schematic illustration of the in situ formation process of the Zn₃(PO₄)₂/ZnF₂-rich SEI and the Zn deposition during cycling. Reproduced with permission from Ref. [135]. Copyright (2021) Royal Society of Chemistry.

decomposition, directly reducing corrosion. Zinc alloying can increase the hydrogen evolution overpotential and thermodynamic stability with the addition of alloying elements. Electro-deposition technology offers improved corrosion resistance of zinc electrodes by forming a controlled and uniform morphology. Coating treatments have different corrosion inhibition mechanisms with acting as a physical isolator to reduce direct contact with water and homogenize the Zn²⁺ deposition. Although decent development has been achieved in zinc anti-corrosion, there are still some issues worthy of consideration and development, which are briefly summarized as shown in Figure 19.

(1) About zinc anode. The performance of zinc anode poses a direct impact on the service life of the battery. With the widespread use of commercial zinc foil, a series of operations such as grinding, polishing and acid etching are required to strive for the best possible surface condition. However, these simple processes cannot change the utilization of zinc anode, and more attention should be paid to maximizing the depth of discharge of the zinc anode without loss of capacity. Although new three-dimensional zinc anodes have been designed, there may be side effects from the increased specific surface area. With this in mind, the strategy of electrodeposition of zinc has not lost its development, and the electrodeposition of small

amounts of zinc on selected substrates brings high zinc utilization. The continuous exploration of new zinc anode structure design is expected to achieve the ideal zinc anode from the ground up.

- (2) About electrolyte additives. Firstly, advanced characterization tests should be combined with basic theoretical simulations to investigate the subtle interactions between electrolyte additives and electrolytes, and to elucidate the intrinsic link between structure and performance of hybrid systems. Secondly, the research on compound electrolyte additives is still in its initial stage, but the efficacy of the compound additives is remarkable, which may be a potential way to compensate for the functional deficiencies of a single electrolyte additive, and how to fully understand the relationship between the types and concentrations of the components of the compound additives is important for the future development of new compound additives. Finally, the timeliness of electrolyte additives should be given more attention. Considering the ever-changing nature of electrolyte parameters, electrolyte additives should be utilized with due consideration to long-lasting functional stability to cope with harsh environments.
- (3) About zinc alloying. The deep theoretical and technical background of metallurgy makes zinc alloying the most promising method for large-scale preparation. Zinc alloys

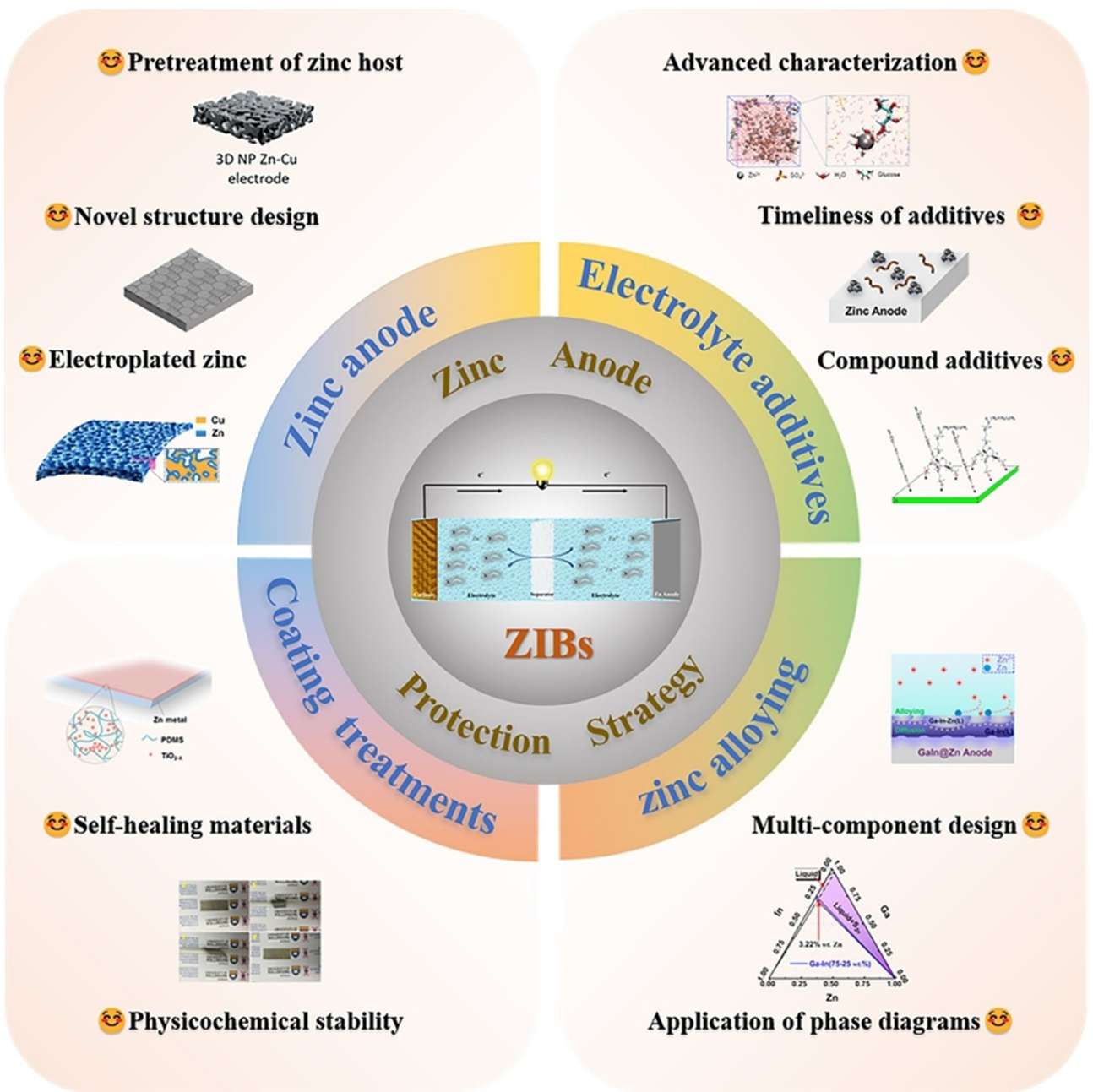


Figure 19. Schematic illustration of zinc anode protection strategies.

for zinc ion batteries have been studied for a long time and these studies have shown that the electrochemical properties of the alloys depend on the chemical composition and phase composition. However, the current studies have been almost exclusively on binary alloy systems and subsequently more alloy systems with different compositions should be considered. With the help of phase diagrams and DFT calculations, it is possible to predict the bonding of zinc with other metals and to select the appropriate metal as a substrate or alloy component for deposition in order to obtain zinc anodes with a homogeneous coating.

- (4) About coating treatments. Although various coatings have been used ever since thanks to the simple effectiveness, further technical optimization of the means is needed. The choice of coating thickness is important for simultaneous corrosion protection and ion transport. It is notable that how to ensure the physicochemical stability of the coating during electrochemical cycling is worthy of deep consideration, and more experiments and simulations are necessary to confirm the reliability of the coating. Fortunately, self-healing materials appear to be a hot topic of research at this stage, and the successful application of self-healing coating for filling surface corrosion pits due to interfacial

parasitic reactions may make a significant contribution to the study of zinc corrosion.

Acknowledgements

This work was financially supported by the National Natural Science Foundation of China (51871138, U2102212 and 22075171), the Science and Technology Committee of Shanghai (19010500400), the Shanghai Rising-Star Program (21QA1403200).

Conflict of Interest

The authors declare no conflict of interest.

Keywords: Fundamental principle • Perspective • Zn anode • Zn-based battery • Zn corrosion

- [1] Y. Lyu, Y. Liu, Z. E. Yu, N. Su, Y. Liu, W. Li, Q. Li, B. Guo, B. Liu, *Sustain. Mater. Technol.* **2019**, 21, e00098.
- [2] Y. Guo, Y. Shi, R. Yuan, H. Leng, Q. Li, *J. Alloys Compd.* **2021**, 873, 159826.
- [3] L. Wang, X. Zhang, S. Zhou, J. Xu, H. Yan, Q. Luo, Q. Li, *Int. J. Hydrogen Energy* **2020**, 45, 16677.
- [4] Y. Ma, T. Zhang, W. He, Q. Luo, Z. Li, W. Zhang, J. He, Q. Li, *Int. J. Hydrogen Energy* **2020**, 45, 12048.
- [5] Y. Shi, H. Leng, L. Wei, S. Chen, Q. Li, *Electrochim. Acta* **2019**, 296, 18.
- [6] Y. Shi, H. Leng, Q. Luo, S. Chen, Q. Li, *Catal. Today* **2018**, 318, 86.
- [7] K. Wu, J. Huang, J. Yi, X. Liu, Y. Liu, Y. Wang, J. Zhang, Y. Xia, *Adv. Energy Mater.* **2020**, 10, 1903977.
- [8] Q. Luo, Y. Guo, B. Liu, Y. Feng, J. Zhang, Q. Li, K. Chou, *J. Mater. Sci. Technol.* **2020**, 44, 171.
- [9] X. Liu, Y. Fang, P. Liang, J. Xu, B. Xing, K. Zhu, Y. Liu, J. Zhang, J. Yi, *Chin. Chem. Lett.* **2021**, 32, 2899.
- [10] Q. Li, X. Lin, Q. Luo, Y. Chen, J. Wang, B. Jiang, F. Pan, *Int. J. Miner. Metall. Mater.* **2022**, 29, 32.
- [11] Q. Li, Y. Lu, Q. Luo, X. Yang, Y. Yang, J. Tan, Z. Dong, J. Dang, J. Li, Y. Chen, B. Jiang, S. Sun, F. Pan, *J. Magnes. Alloy.* **2021**, 9, 1922.
- [12] X. Xie, S. Liang, J. Gao, S. Guo, J. Guo, C. Wang, G. Xu, X. Wu, G. Chen, J. Zhou, *Energy Environ. Sci.* **2020**, 13, 503.
- [13] B. Li, X. Zhang, T. Wang, Z. He, B. Lu, S. Liang, J. Zhou, *Nano-Micro Lett.* **2021**, 14, 6.
- [14] J. Cui, Z. Guo, J. Yi, X. Liu, K. Wu, P. Liang, Q. Li, Y. Liu, Y. Wang, Y. Xia, J. Zhang, *ChemSusChem* **2020**, 13, 2160.
- [15] K. Wu, J. Yi, X. Liu, Y. Sun, J. Cui, Y. Xie, Y. Liu, Y. Xia, J. Zhang, *Nano-Micro Lett.* **2021**, 13, 79.
- [16] R. Hu, Y. Fang, X. Liu, K. Zhu, D. Cao, J. Yi, G. Wang, *Chem. Res. Chin. Univ.* **2021**, 37, 311.
- [17] F. Tang, J. Gao, Q. Ruan, X. Wu, X. Wu, T. Zhang, Z. Liu, Y. Xiang, Z. He, X. Wu, *Electrochim. Acta* **2020**, 353, 136570.
- [18] J. Muldoon, C. B. Bucur, T. Gregory, *Chem. Rev.* **2014**, 114, 11683.
- [19] J. Hao, X. Li, X. Zeng, D. Li, J. Mao, Z. Guo, *Energy Environ. Sci.* **2020**, 13, 3917.
- [20] Q. Li, X. Peng, F. Pan, *J. Magnes. Alloy.* **2021**, 9, 2223.
- [21] T. Wang, C. Li, X. Xie, B. Lu, Z. He, S. Liang, J. Zhou, *ACS Nano* **2020**, 14, 16321.
- [22] X. Liu, J. Yi, K. Wu, Y. Jiang, Y. Liu, B. Zhao, W. Li, J. Zhang, *Nanotechnology* **2020**, 31, 122001.
- [23] D. Chao, W. Zhou, F. Xie, C. Ye, H. Li, M. Jaroniec, S. Z. Qiao, *Sci. Adv.* **2020**, 6, eaba4098.
- [24] N. Zhang, X. Chen, M. Yu, Z. Niu, F. Cheng, J. Chen, *Chem. Soc. Rev.* **2020**, 49, 4203.
- [25] L. E. Blanc, D. Kundu, L. F. Nazar, *Joule* **2020**, 4, 771.
- [26] J. Yi, P. Liang, X. Liu, K. Wu, Y. Liu, Y. Wang, Y. Xia, J. Zhang, *Energy Environ. Sci.* **2018**, 11, 3075.
- [27] H. Wei, X. Hu, X. Zhang, Z. Yu, T. Zhou, Y. Liu, Y. Liu, Y. Wang, J. Xie, L. Sun, M. Liang, P. Jiang, *Energy Technol.* **2019**, 7, 1800912.
- [28] M. H. Lin, C. J. Huang, P. H. Cheng, J. H. Cheng, C. C. Wang, *J. Mater. Chem. A* **2020**, 8, 20637.
- [29] L. L. Lei, Y. T. Sun, X. Y. Wang, Y. M. Jiang, J. Li, *Front. Mater.* **2020**, 7,
- [30] T. K. A. Hoang, T. N. L. Doan, K. E. K. Sun, P. Chen, *RSC Adv.* **2015**, 5, 41677.
- [31] A. Bayaguud, Y. Fu, C. Zhu, *J. Energy Chem.* **2022**, 64, 246.
- [32] N. Zhang, F. Cheng, Y. Liu, Q. Zhao, K. Lei, C. Chen, X. Liu, J. Chen, *J. Am. Chem. Soc.* **2016**, 138, 12894.
- [33] L. Wang, S. Han, H. Zhang, W. Wang, L. Zhang, *Acta Chim. Sin.* **2021**, 79, 158.
- [34] C. Li, X. Xie, S. Liang, J. Zhou, *Energy Environ. Mater.* **2020**, 3, 146.
- [35] S. Thomas, N. Birbilis, M. S. Venkatraman, I. S. Cole, *Corrosion* **2012**, 68, 015009.
- [36] P. He, J. Huang, *ACS Energy Lett.* **2021**, 6, 1990.
- [37] K. Chen, J. Han, X. Pan, D. J. Srolovitz, *Proc. Natl. Acad. Sci. USA* **2020**, 117, 4533.
- [38] Z. Zhang, S. Said, K. Smith, Y. S. Zhang, G. He, R. Jervis, P. R. Shearing, T. S. Miller, D. J. L. Brett, *J. Mater. Chem. A* **2021**, 9, 15355.
- [39] Z. Yu, A. T. O. Lim, S. L. Kollasch, H. D. Jang, J. Huang, *Adv. Funct. Mater.* **2020**, 30, 1906273.
- [40] M. Mouanga, P. Berçot, J. Y. Rauch, *Corros. Sci.* **2010**, 52, 3984.
- [41] M. Zhou, Y. Chen, G. Fang, S. Liang, *Energy Storage Mater.* **2022**, 45, 618.
- [42] J. Zheng, A. Archer Lynden, *Sci. Adv.* **2021**, 7, eabe0219.
- [43] C. Han, W. Li, H. K. Liu, S. Dou, J. Wang, *Nano Energy* **2020**, 74, 104880.
- [44] Z. Li, L. Wu, S. Dong, T. Xu, S. Li, Y. An, J. Jiang, X. Zhang, *Adv. Funct. Mater.* **2021**, 31, 2006495.
- [45] J. Hao, X. Li, S. Zhang, F. Yang, X. Zeng, S. Zhang, G. Bo, C. Wang, Z. Guo, *Adv. Funct. Mater.* **2020**, 30, 2001263.
- [46] Z. Cao, X. Zhu, D. Xu, P. Dong, M. O. L. Chee, X. Li, K. Zhu, M. Ye, J. Shen, *Energy Storage Mater.* **2021**, 36, 132.
- [47] L. Zhang, I. A. Rodríguez-Pérez, H. Jiang, C. Zhang, D. P. Leonard, Q. Guo, W. Wang, S. Han, L. Wang, X. Ji, *Adv. Funct. Mater.* **2019**, 29, 1902653.
- [48] X. Zeng, K. Xie, S. Liu, S. Zhang, J. Hao, J. Liu, W. K. Pang, J. Liu, P. Rao, Q. Wang, J. Mao, Z. Guo, *Energy Environ. Sci.* **2021**, 14, 5947.
- [49] Y. Dong, M. Jia, Y. Wang, J. Xu, Y. Liu, L. Jiao, N. Zhang, *ACS Appl. Energ. Mater.* **2020**, 3, 11183.
- [50] Z. Cai, Y. Ou, J. Wang, R. Xiao, L. Fu, Z. Yuan, R. Zhan, Y. Sun, *Energy Storage Mater.* **2020**, 27, 205.
- [51] M. Li, Z. L. Li, X. P. Wang, J. S. Meng, X. Liu, B. K. Wu, C. H. Han, L. Q. Mai, *Energy Environ. Sci.* **2021**, 14, 3796.
- [52] X. Tang, P. Wang, M. Bai, Z. Wang, H. Wang, M. Zhang, Y. Ma, *Adv. Sci.* **2021**, 8, e2102053.
- [53] F. Wang, O. Borodin, T. Gao, X. Fan, W. Sun, F. Han, A. Faraone, J. A. Dura, K. Xu, C. Wang, *Nat. Mater.* **2018**, 17, 543.
- [54] L. Cao, D. Li, E. Hu, J. Xu, T. Deng, L. Ma, Y. Wang, X. Q. Yang, C. Wang, *J. Am. Chem. Soc.* **2020**, 142, 21404.
- [55] C. Zhang, J. Holoubek, X. Wu, A. Daniyar, L. Zhu, C. Chen, D. P. Leonard, I. A. Rodríguez-Pérez, J. X. Jiang, C. Fang, X. Ji, *Chem. Commun.* **2018**, 54, 14097.
- [56] J. Zhao, J. Zhang, W. Yang, B. Chen, Z. Zhao, H. Qiu, S. Dong, X. Zhou, G. Cui, L. Chen, *Nano Energy* **2019**, 57, 625.
- [57] J. Ming, J. Guo, C. Xia, W. Wang, H. N. Alshareef, *Mater. Sci. Eng. R-Rep.* **2019**, 135, 58.
- [58] A. Konarov, N. Voronina, J. H. Jo, Z. Bakenov, Y. K. Sun, S. T. Myung, *ACS Energy Lett.* **2018**, 3, 2620.
- [59] J. Fu, Z. P. Cano, M. G. Park, A. Yu, M. Fowler, Z. Chen, *Adv. Mater.* **2017**, 29, 1604685.
- [60] M. Pourbaix, *NACE 1974*, 307, 407.
- [61] B. Zhang, Y. Liu, X. Wu, Y. Yang, Z. Chang, Z. Wen, Y. Wu, *Chem. Commun.* **2014**, 50, 1209.
- [62] W. Kaveevivitchai, A. Manthiram, *J. Mater. Chem. A* **2016**, 4, 18737.
- [63] G. Li, Z. Yang, Y. Jiang, W. Zhang, Y. Huang, *J. Power Sources* **2016**, 308, 52.
- [64] Z. Guo, Y. Ma, X. Dong, J. Huang, Y. Wang, Y. Xia, *Angew. Chem. Int. Ed.* **2018**, 57, 11737.
- [65] F. Wan, L. Zhang, X. Dai, X. Wang, Z. Niu, J. Chen, *Nat. Commun.* **2018**, 9, 1656.
- [66] C. Zhu, G. Fang, J. Zhou, J. Guo, Z. Wang, C. Wang, J. Li, Y. Tang, S. Liang, *J. Mater. Chem. A* **2018**, 6, 9677.
- [67] Z. Peng, Q. Wei, S. Tan, P. He, W. Luo, Q. An, L. Mai, *Chem. Commun.* **2018**, 54, 4041.

- [68] P. Hu, T. Zhu, X. Wang, X. Zhou, X. Wei, X. Yao, W. Luo, C. Shi, K. A. Owusu, L. Zhou, L. Mai, *Nano Energy* **2019**, *58*, 492.
- [69] J. Lai, H. Zhu, X. Zhu, H. Koritala, Y. Wang, *ACS Appl. Energ. Mater.* **2019**, *2*, 1988.
- [70] B. Lan, Z. Peng, L. Chen, C. Tang, S. Dong, C. Chen, M. Zhou, C. Chen, Q. An, P. Luo, *J. Alloys Compd.* **2019**, *787*, 9.
- [71] C. Xie, Y. Li, Q. Wang, D. Sun, Y. Tang, H. Wang, *Carbon Energy* **2020**, *2*, 540.
- [72] K. Wippermann, J. W. Schultze, R. Kessel, J. Penninger, *Corros. Sci.* **1991**, *32*, 205.
- [73] X. G. Zhang, *Corrosion and electrochemistry of zinc*, Springer Science & Business Media 1996.
- [74] W. He, S. Zuo, X. Xu, L. Zeng, L. Liu, W. Zhao, J. J. M. C. F. Liu, *Mat. Chem. Front.* **2021**, *5*, 2201.
- [75] S. Guo, L. Qin, T. Zhang, M. Zhou, J. Zhou, G. Fang, S. Liang, *Energy Storage Mater.* **2021**, *34*, 545.
- [76] K. E. K. Sun, T. K. A. Hoang, T. N. L. Doan, Y. Yu, P. Chen, *Chem. Eur. J.* **2018**, *24*, 1667.
- [77] D. Mackinnon, J. Brannen, P. J. J. o. a. e. Fenn, *J. Appl. Electrochem.* **1987**, *17*, 1129.
- [78] A. Gomes, M. I. da Silva Pereira, *Electrochim. Acta* **2006**, *51*, 1342.
- [79] A. Khor, P. Leung, M. R. Mohamed, C. Flox, Q. Xu, L. An, R. G. A. Wills, J. R. Morante, A. A. Shah, *Mater. Today* **2018**, *8*, 80.
- [80] K. M. Youssef, C. C. Koch, P. S. Fedkiw, *Electrochim. Acta* **2008**, *54*, 677.
- [81] T. Otani, Y. Fukunaka, T. Homma, *Electrochim. Acta* **2017**, *242*, 364.
- [82] K. E. K. Sun, T. K. A. Hoang, T. N. L. Doan, Y. Yu, X. Zhu, Y. Tian, P. Chen, *ACS Appl. Mater. Interfaces* **2017**, *9*, 9681.
- [83] G. Trejo, H. Ruiz, R. O. Borges, Y. Meas, *J. Appl. Electrochem.* **2001**, *31*, 685.
- [84] J. Hao, J. Long, B. Li, X. Li, S. Zhang, F. Yang, X. Zeng, Z. Yang, W. K. Pang, Z. Guo, *Adv. Funct. Mater.* **2019**, *29*, 1903605.
- [85] H. Yang, Y. Cao, X. Ai, L. Xiao, *J. Power Sources* **2004**, *128*, 97.
- [86] S. J. Banik, R. Akolkar, *Electrochim. Acta* **2015**, *179*, 475.
- [87] A. Bayaguu, X. Luo, Y. Fu, C. Zhu, *ACS Energy Lett.* **2020**, *5*, 3012.
- [88] S. Hosseini, W. Lao Atiman, S. J. Han, A. Arporntwichanop, T. Yonezawa, S. Kheawhom, *Sci. Rep.* **2018**, *8*, 14909.
- [89] Z. Hou, X. Zhang, X. Li, Y. Zhu, J. Liang, Y. Qian, *J. Mater. Chem. A* **2017**, *5*, 730.
- [90] A. Mitha, A. Z. Yazdi, M. Ahmed, P. Chen, *ChemElectroChem* **2018**, *5*, 2409.
- [91] J. Zhu, Y. Zhou, *J. Power Sources* **1998**, *73*, 266.
- [92] Y. Ein Eli, M. Auinat, D. Starosvetsky, *J. Power Sources* **2003**, *114*, 330.
- [93] J. Dobryszycki, S. Biallozor, *Corros. Sci.* **2001**, *43*, 1309.
- [94] T. Cohen Hyams, Y. Ziengerman, Y. Ein Eli, *J. Power Sources* **2006**, *157*, 584.
- [95] M. Liang, H. Zhou, Q. Huang, S. Hu, W. Li, *J. Appl. Electrochem.* **2011**, *41*, 991.
- [96] H. Zhou, Q. Huang, M. Liang, D. Lv, M. Xu, H. Li, W. Li, *Mater. Chem. Phys.* **2011**, *128*, 214.
- [97] C. W. Lee, K. Sathiyaranayanan, S. W. Eom, H. S. Kim, M. S. Yun, *J. Power Sources* **2006**, *159*, 1474.
- [98] M. C. Li, S. Z. Luo, Y. H. Qian, W. Q. Zhang, L. L. Jiang, J. N. Shen, *J. Electrochem. Soc.* **2007**, *154*, D567.
- [99] J. Cui, X. Liu, Y. Xie, K. Wu, Y. Wang, Y. Liu, J. Zhang, J. Yi, Y. Xia, *Mater. Today Energy* **2020**, *18*, 100563.
- [100] J. Q. Huang, X. W. Chi, Q. Han, Y. Z. Liu, Y. X. Du, J. H. Yang, Y. Liu, *J. Electrochem. Soc.* **2019**, *166*, A1211.
- [101] P. Sun, L. Ma, W. Zhou, M. Qiu, Z. Wang, D. Chao, W. Mai, *Angew. Chem. Int. Ed.* **2021**, *60*, 18247.
- [102] D. Feng, F. Cao, L. Hou, T. Li, Y. Jiao, P. Wu, *Small* **2021**, *17*, 2103195.
- [103] D. Han, S. Wu, S. Zhang, Y. Deng, C. Cui, L. Zhang, Y. Long, H. Li, Y. Tao, Z. Weng, Q. H. Yang, F. Kang, *Small* **2020**, *16*, 2001736.
- [104] B. Liu, S. Wang, Z. Wang, H. Lei, Z. Chen, W. Mai, *Small* **2020**, *16*, 2001323.
- [105] S. B. Wang, Q. Ran, R. Q. Yao, H. Shi, Z. Wen, M. Zhao, X. Y. Lang, Q. Jiang, *Nat. Commun.* **2020**, *11*, 1634.
- [106] X. Fan, H. Yang, X. Wang, J. Han, Y. Wu, L. Gou, D. L. Li, Y. L. Ding, *Adv. Mater. Interfaces* **2021**, *8*, 2002184.
- [107] Z. Y. Miao, M. Du, H. Z. Li, F. Zhang, H. C. Jiang, Y. H. Sang, Q. F. Li, H. Liu, S. H. Wang, *Ecomat* **2021**, *3*, 1.
- [108] Z. Qi, T. Xiong, T. Chen, C. Yu, M. Zhang, Y. Yang, Z. Deng, H. Xiao, W. S. V. Lee, J. Xue, *ACS Appl. Mater. Interfaces* **2021**, *13*, 28129.
- [109] L. Zhang, B. Zhang, T. Zhang, T. Li, T. Shi, W. Li, T. Shen, X. Huang, J. Xu, X. Zhang, Z. Wang, Y. Hou, *Adv. Funct. Mater.* **2021**, *31*, 2100186.
- [110] Y. Zhang, J. D. Howe, S. Ben-Yoseph, Y. Wu, N. Liu, *ACS Energy Lett.* **2021**, *6*, 404.
- [111] C. Liu, Z. Luo, W. Deng, W. Wei, L. Chen, A. Pan, J. Ma, C. Wang, L. Zhu, L. Xie, X. Y. Cao, J. Hu, G. Zou, H. Hou, X. Ji, *ACS Energy Lett.* **2021**, *6*, 675.
- [112] L. Wang, W. Huang, W. Guo, Z. H. Guo, C. Chang, L. Gao, X. Pu, *Adv. Funct. Mater.* **2021**, *32*, 2108533.
- [113] Y. Wang, Y. Chen, W. Liu, X. Ni, P. Qing, Q. Zhao, W. Wei, X. Ji, J. Ma, L. Chen, *J. Mater. Chem. A* **2021**, *9*, 8452.
- [114] A. Koyama, K. Fukami, Y. Suzuki, A. Kitada, T. Sakka, T. Abe, K. Murase, M. Kinoshita, *J. Phys. Chem. C* **2016**, *120*, 24112.
- [115] Z. Wu, X. Yuan, M. Jiang, L. Wang, Q. Huang, L. Fu, Y. Wu, *Energy Fuels* **2020**, *34*, 13118.
- [116] L. P. Wang, N. W. Li, T. S. Wang, Y. X. Yin, Y. G. Guo, C. R. Wang, *Electrochim. Acta* **2017**, *244*, 172.
- [117] Q. Zhang, J. Luan, L. Fu, S. Wu, Y. Tang, X. Ji, H. Wang, *Angew. Chem. Int. Ed.* **2019**, *58*, 15841.
- [118] Z. Kang, C. Wu, L. Dong, W. Liu, J. Mou, J. Zhang, Z. Chang, B. Jiang, G. Wang, F. Kang, C. Xu, *ACS Sustainable Chem. Eng.* **2019**, *7*, 3364.
- [119] Y. Huang, Z. Chang, W. Liu, W. Huang, L. Dong, F. Kang, C. Xu, *Chem. Eng. J.* **2022**, *431*, 133902.
- [120] W. Du, E. H. Ang, Y. Yang, Y. Zhang, M. Ye, C. C. Li, *Energy Environ. Sci.* **2020**, *13*, 3330.
- [121] B. Li, J. Xue, C. Han, N. Liu, K. Ma, R. Zhang, X. Wu, L. Dai, L. Wang, Z. He, *J. Colloid Interface Sci.* **2021**, *599*, 467.
- [122] L. Kang, M. Cui, F. Jiang, Y. Gao, H. Luo, J. Liu, W. Liang, C. Zhi, *Adv. Energy Mater.* **2018**, *8*, 1801090.
- [123] C. Deng, X. Xie, J. Han, Y. Tang, J. Gao, C. Liu, X. Shi, J. Zhou, S. Liang, *Adv. Funct. Mater.* **2020**, *30*, 2000599.
- [124] P. Liang, J. Yi, X. Liu, K. Wu, Z. Wang, J. Cui, Y. Liu, Y. Wang, Y. Xia, J. Zhang, *Adv. Funct. Mater.* **2020**, *30*, 1908528.
- [125] K. Zhao, C. Wang, Y. Yu, M. Yan, Q. Wei, P. He, Y. Dong, Z. Zhang, X. Wang, L. Mai, *Adv. Mater. Interfaces* **2018**, *5*, 1800848.
- [126] J. Shin, J. Lee, Y. Kim, Y. Park, M. Kim, J. W. Choi, *Adv. Energy Mater.* **2021**, *11*, 2100676.
- [127] S. H. Park, S. Y. Byeon, J. H. Park, C. Kim, *ACS Energy Lett.* **2021**, *6*, 3078.
- [128] D. Lee, H. I. Kim, W. Y. Kim, S. K. Cho, K. Baek, K. Jeong, D. B. Ahn, S. Park, S. J. Kang, S. Y. Lee, *Adv. Funct. Mater.* **2021**, *31*, 2103850.
- [129] Y. Jiao, F. Li, X. Jin, Q. Lei, L. Li, L. Wang, T. Ye, E. He, J. Wang, H. Chen, J. Lu, R. Gao, Q. Li, C. Jiang, J. Li, G. He, M. Liao, H. Zhang, I. P. Parkin, H. Peng, Y. Zhang, *Adv. Funct. Mater.* **2021**, *31*, 2107652.
- [130] Z. Guo, L. Fan, C. Zhao, A. Chen, N. Liu, Y. Zhang, N. Zhang, *Adv. Mater.* **2022**, *34*, e2105133.
- [131] A. Wang, W. Zhou, A. Huang, M. Chen, J. Chen, Q. Tian, J. Xu, *J. Colloid Interface Sci.* **2020**, *577*, 256.
- [132] Z. Zhao, J. Zhao, Z. Hu, J. Li, J. Li, Y. Zhang, C. Wang, G. Cui, *Energy Environ. Sci.* **2019**, *12*, 1938.
- [133] L. Ma, Q. Li, Y. Ying, F. Ma, S. Chen, Y. Li, H. Huang, C. Zhi, *Adv. Mater.* **2021**, *33*, 2007406.
- [134] J. Hao, B. Li, X. Li, X. Zeng, S. Zhang, F. Yang, S. Liu, D. Li, C. Wu, Z. Guo, *Adv. Mater.* **2020**, *32*, 2003021.
- [135] Y. Z. Chu, S. Zhang, S. Wu, Z. L. Hu, G. L. Cui, J. Y. Luo, *Energy Environ. Sci.* **2021**, *14*, 3609.
- [136] S. Di, X. Nie, G. Ma, W. Yuan, Y. Wang, Y. Liu, S. Shen, N. Zhang, *Energy Storage Mater.* **2021**, *43*, 375.

Manuscript received: December 28, 2021

Revised manuscript received: January 23, 2022

Version of record online: February 9, 2022